CATALYTIC IGNITION OF AQUANOL

FINAL REPORT

OCTOBER 2002

Report Budget Number KLK319
NIATT Report N02-06A

Prepared for

OFFICE OF UNIVERSITY RESEARCH AND EDUCATION

U.S. DEPARTMENT OF TRANSPORTATION

Prepared by

NATIONAL INSTITUTE FOR ADVANCED TRANSPORTATION TECHNOLOGY

UNIVERSITY OF IDAHO

Judi Steciak, PhD, PE
Steve Beyerlein, PhD
with
Eric Clarke, Dan Cordon, Amit Patel, Xiangyang Wang, and Jeff Williams

TABLE OF CONTENTS

EXECUTIVE SUMMARY

Aqueous fueled engines have the potential for lower emissions and higher engine efficiency than engines fueled with gasoline or diesel engines. Past attempts to burn aqueous fuels in over-the-road vehicles have been unsuccessful due to difficulties in initiating combustion under varying environmental conditions. Ethanol-water mixtures, called Aquanol, require no special emulsifications to create and should provide significant emission reductions in carbon monoxide (CO) and nitrous oxide (NOx,) while producing no net carbon dioxide (CO_2) emissions. Aldehydes, a part of the hydrocarbon emissions, are expected to increase with alcohol-based fuels. Understanding the parameters that affect aldehyde formation will help create reduction strategies. Detailed detection of exhaust emissions is necessary for a quantitative comparison.

Redundant measurements with two special purpose detectors were used for emission comparisons. A van supplied by Valley Transit of Lewiston, Idaho was converted to catalytic ignition. Modifications to the fuel handling, engine management, and ignition system were necessary to make the vehicle operate on either gasoline or Aquanol. A three-part vehicle test plan is currently underway to compare performance, fuel economy, and emissions between Aquanol and gasoline fuels.

In the catalytically ignited ethanol-water system, ignition timing can be adjusted by changing the length of the catalytic core element, the length of the pre-chamber, the diameter of the pre-chamber, and the electrical power supplied to the catalytic core element.

A multi-zone energy balance model has been developed to understand ignition timing of ethanol-water mixtures. Model predictions agree with pressure versus crank angle data obtained from a 15 kW Yanmar diesel engine converted for catalytic operation on ethanol-water fuel. Comparing the converted Yanmar to the stock engine shows an

increase in torque and power, with improvements in CO and NOx emissions. Hydrocarbon emissions increased significantly, but are largely due to piston geometry not well suited for homogeneous charge combustion. Future engine modifications have the potential to lower emissions to current emission standards, without requiring external emission control devices.

A catalytic plug flow reactor is being built to better understand the heterogeneous combustion of ethanol-water-air mixtures. A key feature is the reactor's ability to rapidly mix fuel vapor and air streams. A prototype mixing nozzle, designed and built last year, was evaluated using gas streams of two different compositions.

The chemical kinetic's code HCT (hydrodynamics, combustion and transport), developed by Lawrence Livermore National Laboratory, is being used to model gas-phase combustion of ethanol-water-air mixtures. A literature search of surface reaction mechanisms was performed. HCT will be modified to accommodate surface reactions, and thus be available as a tool for better understanding of catalytic ignition of aqueous ethanol.

DESCRIPTION OF PROBLEM

Our support of the development of a catalytic igniter for lean-burning aqueous ethanol follows three parallel paths: testing of demonstration vehicles, stand-alone engine testing and igniter modeling, and fundamental studies of oxidative catalysis with experimentation and detailed chemical kinetic modeling.

Demonstration vehicles are needed for actual use experience and public awareness. Engine work is helping to develop a first order model of catalytic ignition to assist igniter design. Fundamental studies improve our understanding of the underlying chemistry and physics.

Results of our efforts in are presented in the following three sections:

A. Vehicle Testing
B. Engine Testing and Igniter Modeling
C. Ethanol-Water Combustion Kinetics

A. VEHICLE TESTING

Approach and Methodology

To demonstrate the potential of Aquanol as a feasible alternative fuel, a gasoline V8 powered van was converted to run on either Aquanol or gasoline. Testing compared emissions, thermal efficiency, and power between the two fuels, both before and after catalytic converter cleanup.

The University of Idaho and Automotive Resources, Inc. have been working with Aquanol fueled engines since 1996. Aquanol is a mix of 65 percent ethanol and 35 percent water. Engines have run on mixtures up to 50 percent ethanol and 50 percent water, and shown cold starting capabilities unmatched in the literature. Previous testing on diesel conversions show significant reductions in NOx and CO, and have promise of lower HC emissions when compared to the same unconverted platform.

Increasing public awareness of alternative fuels is another goal of this research. Therefore, the vehicle was enhanced cosmetically to display information about this technology (Fig. 1). The vehicle is driven locally, and displayed at conferences and events. Eventually, this technology will be used in a local public transit system.

Figure 1. The dual fuel conversion platform

1. *Aquanol Emissions*

Information about emissions of lean burn engines, alcohol fueled engines, and the effects of water on emissions are readily found in the literature. What is generally not available is work that addresses all three topics. This section outlines expected emissions from a lean burn Aquanol engine.

Major Emissions Constituents

Carbon Monoxide (CO) is one of the major species regulated in vehicle applications. CO emissions in gasoline engines are usually formed under two conditions. Engines running rich will produce significantly more CO than one running near stoichiometric or excess air conditions [1]. A second condition that produces larger quantities of CO is misfire, or incomplete combustion. Depending on the source, simply switching from gasoline to ethanol will net a 24-50 percent decrease in CO emissions [2, 3]. Also, the dominant mechanism for CO destruction involves the "water-gas shift mechanism," where increasing the water concentration in the exhaust will increase the amount of CO converted to CO_2. Because the Aquanol conversion runs lean and is a water-ethanol mix, we expect the Aquanol conversion to see a reduction in CO emissions of 25-60 percent.

Carbon dioxide (CO_2) emissions of Aquanol engines have huge benefits over their gasoline counterparts. Because ethanol is a product of renewable sources, the net CO_2 for the fuel is zero, regardless of the CO_2 output of the engine, because the maximum amount of CO_2 produced by combustion is equal to the amount of CO_2 absorbed by the fuel source before being turned into ethanol. However, because of the expected increase in fuel consumption, amounts of CO_2 measured in the exhaust stream will likely increase by as much as 20 percent.

Nitrous Oxide (NOx) is difficult to clean up with after-treatment systems, so reducing the formation of NOx was a primary goal for the Aquanol conversion. The formation of NOx is a drawback of typical lean burn engines. It also has a strong dependence on

combustion temperatures [4]. Although gasoline engines emit lower NOx than diesel engines, gasoline engines still require clean up to comply with future emission standards. Engines converted to run on E85 typically show a NOx reduction of 20-25 percent [2, 5]. However, because of the added water in Aquanol, combustion temperatures are much lower than E85, and a further reduction of NOx is expected in the range of 50-75 percent.

Hydrocarbon (HC) emissions are usually due to unburnt fuel that has escaped combustion. While excessive levels of HC are produced from rich burning engines, lean burn engines can still suffer from high HC emissions that comes from three different sources. First, the crevices in the engine around spark plugs and between the cylinder wall and piston are too small for the flame to propagate. Even if oxygen is available, the fuel in this region will not ignite. A second source of HC production is the oil on the cylinder wall. The thin film of oil will absorb some of the fuel and keep it from combusting. The third source of HC is from cold starting. Single reducing catalytic converters do an excellent job of burning up HC in the exhaust, but only after they have reached operating temperatures. This is commonly called “light-off time.” Reducing light-off time has a positive effect on lowering HC emissions. Most catalytic converters rely on the latent energy in the exhaust to heat to operating temperatures. Because the Aquanol engines have much lower exhaust temperatures, catalytic converter light-off will likely take longer. Because of this, an expected increase in HC production will likely be in the 20-35 percent range.

Adehyde Formation

In the 1970s, alcohols gained popularity as an alternative fuel. Both methanol and ethanol can be produced from renewable resources. General exhaust emissions of CO and HC were on a similar level as gasoline engines, while NOx was lower [6]. However, aldehyde emissions increased by a factor of four to ten. Because aldehydes are an insignificant part of gasoline emissions, they are currently unregulated. As alcohol fuel becomes more prevalent, this is certain to change. Any combusted alcohol

will produce aldehydes. Methanol fuel tends to primarily produce formaldehyde, while ethanol forms acetaldehyde. Both species show up as part of hydrocarbon emissions, but demonstrate higher reactivity in photochemical smog formation than other hydrocarbons. Before alcohol fuel can become widely adopted, aldehyde emissions need to be reduced. Accurate characterization of when and where aldehydes are formed is necessary to design a scheme for their reduction.

Oxidation studies on hydrocarbon fuels show that the reactions proceed through two parallel paths [7]. In the combustion of hydrocarbon fuels, only one of the paths involves the formation of aldehydes. Conversely, in the combustion of alcohol fuels, the intermediate paths are always through aldehyde formation. This partially explains why alcohols produce more aldehyde emissions.

TABLE 1 Key reactions in the formation and destruction of formaldehyde

Forming	Destroying
$CH_2OH + O_2 = CH_2O + HO_2$ (1)	$CH_2O + OH = CHO + H_2O$ (5)
$CH_2OH + M = CH_2O + H + M$ (2)	$CH_2O + H = CHO + H_2$ (6)
$CH_3 + O_2 = CH_2O + OH$ (3)	$CH_2O + M = CO + H_2 + M$ (7)
$CH_3 + O = CH_2O + H$ (4)	

Aldehydes were believed to be most prominent in the quench zone, and a detailed kinetics model was made to predict emissions. Browning and Pefley conducted a series of studies on aldehyde formation from methanol [8, 9] and identified a reaction set of 94 reactions, along with their respective forward reaction rates. Key reactions at temperatures found in combustion are shown in Table 1 [10]. Of the two primary paths for formation, one goes through hydroxymethyl radical (CH_2OH), and the other through methyl radical (CH_3). The first reaction accounts for nearly all the consumption of CH_2OH. These equations suggest that molecular oxygen in the

exhaust can lead to formaldehyde formation, while presence of hydroxyl and hydrogen radicals would have positive effects on formaldehyde destruction.
Results of the Browning and Pefley model were compared to experimental results. Calculated quench distances agreed nicely with two-plate quench experiments. However, the predicted concentrations of HC and aldehydes in the exhaust were not in agreement with measured concentrations. Predicted HC were ten times higher than actual, while aldehydes were 1/12th of the actual measurement. This was thought to uphold reasoning that HC was oxidized as it was removed from the quench zones where aldehydes form. The aldehydes are not fully consumed due to the freezing of the reaction when the exhaust valve opens.

Several parametric studies on engine parameters, summarized in Table 2, have been conducted that identify the effect of primary and secondary parameters on aldehyde formation [7–15] These include 1) compression ratio, 2) engine speed and load, 3) air/fuel ratio, 4) ignition timing, 5) water content of fuel, 6) engine coolant temperature, and 7) ignition type.

TABLE 2 Trends of Aldehyde formation in parametric studies

Parameter	Impact on Aldehyde formation	Reference
Compression ratio	Increase with increasing compression ratio	[7] [11] [12]
Engine speed	Decrease with increasing engine speed	[9] [13]
Engine load	Increase with increasing load	[9] [13]
Air/fuel ratio	Minimized at stoichiometric	[7] [10]
Ignition timing	Decrease with ignition advance	[10] [12]
Water content	Increased above 10 percent water by volume	[11] [12] [14]
Coolant temperature	Increased with reduced coolant temperature	[8] [9]
Ignition type	Decreased with stronger ignition source	[15]

This information suggests engines with high compression ratio and lean mixtures are prone to high aldehyde emissions. However, the use of water in the fuel with early ignition timing should control emissions to reasonable levels. Future engine modifications could benefit from modifications proven to reduce aldehyde formation.

Emission Detection

With emissions testing, it is often desirable to have redundant measurements. For this reason, the University of Idaho engine emissions lab uses two parallel analyzers. A five-gas analyzer from EMS® monitors concentrations of typical engine exhaust products, and a Fourier Transform Infrared Spectrometer (FTIR) is used for more exotic species. Other components of the emissions test station include a test cell, anemometer, exhaust thermocouple and computer. Both the FTIR and five-gas analyzer pull samples from a test cell as the exhaust flows through.

The five-gas analyzer is a flow-through meter with individual sensors for specific species. Small percentages of the exhaust stream are pulled through a probe placed in the exhaust system and are assumed to be representative of the total mixture in the exhaust stream. Inside reside sensors for oxygen, NOx, CO, CO_2 and unburned hydrocarbons. The unit has its own pump and separate exhaust lines for water and products. The five-gas analyzer requires calibration every few months. Also, electrochemical sensors need replacing every two to five years, depending on the sensor and severity of use.

Emissions data is collected in percent volume of the flow for each species. In order to compare various engine sizes using brake specific normalization, the emissions data is converted to mass flow rate of each species. An anemometer is present in the test section to measure the exhaust velocity through the test cell, which is converted into volumetric flow rate. Using the exhaust temperature and the ideal gas law, densities of each species are obtained. The mass flow rate of the emission species is obtained by

multiplying the volumetric flow rate, percent volume of the species, and density of the species.

While the FTIR is a flow-through devise like the five-gas analyzer, the method of detection differs. A heated pump diverts some of the exhaust stream through insulated lines that help prevent water precipitation. This mixture flows in to a chamber where a laser penetrates the exhaust. A photo detector picks up the intensity spectrum over a frequency range. The frequency band excited and magnitude thereof correspond to a species and concentration. Special computer programs and significant verification were necessary in setting the machine up. Because the test section on the FTIR has significant volume, it is difficult to get good transient response. However, for steady state measurements the volume also acts as a transient buffer.

2. Vehicle Conversion

Conversion of a vehicle to run Aquanol fuel requires the replacement of several engine and fuel handling components. The effort described in this paper applies to the components used in the conversion of a 1985 Ford Extended Van. Not all of the changes made to the vehicle were necessary for conversion, but the diagnostics and detection components are crucial for data collection and troubleshooting when using the van as a research platform. Components used in the conversion are summarized in Table 3.

TABLE 3 Components used to convert to Aquanol fuel

Component	Material	Cost
Catalytic igniters	Brass/ceramic	$400
Larger diameter hard fuel lines and fittings	304 stainless	$500
Auto-flex flexible fuel line and fittings	Stainless/aluminum	$200
Tank switch ball valves	304 Stainless	$325
Fuel pressure regulator	Stainless/aluminum	$200
High-flow fuel pump	Stainless/aluminum	$250

Alcohol compatible fuel injectors	316 Stainless	$800
Programmable fuel computer and wiring	Not applicable	$1200
Aquanol fuel tank	Polyethylene	$200

Catalytic Igniters

Catalytic igniters are a crucial part of the Aquanol conversion. Aquanol has a lower heating value than gasoline and diesel, but requires a stronger ignition source. Traditional spark plugs will not ignite or initiate flame propagation. Catalytic igniters operate using a heated catalyst in a pre-chamber located adjacent to the main chamber. For this conversion, each spark plug was replaced with one catalytic igniter.

The four stages of catalytic ignition are: 1) Fuel decomposition on the catalyst during compression; 2) accumulation of decomposition products and radicals in rear of pre-chamber; 3) compression ignition of remaining mixture in the pre-chamber; and 4) rapid torch ignition of the main chamber. Using catalytic igniters changes the engine to a Homogeneous Charge Compression Ignition (HCCI) configuration. Ignition timing is controlled by changing heat transfer characteristics of the catalyst. Currently, to set ignition timing for various engines, the pre-chamber diameter is changed. Once set, the ignition timing follows a desirable path of advancing with engine speed, but reduces with engine load.

Fuel System

Because the demonstration vehicle was being used to compare gasoline to Aquanol, it had to easily switch from one fuel to the other. When running gasoline, a standard ignition system is used. The fuel delivery system has a return line. When switching fuels, the return line is purged until the newly switched fuel drains. This prevents cross contamination of the fuel tanks.

Aquanol fuel is highly corrosive to many materials traditionally found in gasoline fuel systems. The combination of ethanol and water is many times harsher than either individually. Therefore, any component in contact with the fuel was replaced. Thus

far, only stainless steel and hard-anodized aluminum have shown significant resistance to corrosion. All the fuel lines are plumbed with 304 stainless tubing, with necessary flexible connections made from stainless hose with hard-anodized aluminum fittings. The fuel pump and pressure regulator are also stainless with hard-anodized aluminum housings. These are shown in Figure 2. Tank switch valves are stainless, and the fuel injectors are made with stainless internals. The gasoline fuel tank is a stock steel tank, and needs no modifications. The Aquanol tank is a polypropylene unit. It is being carefully observed for any problems associated with Aquanol storage.

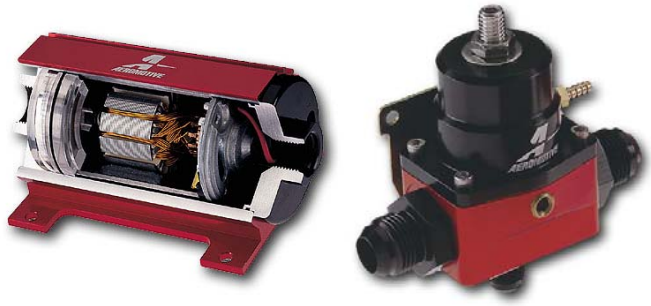

Figure 2. Fuel pump and regulator used in the Aquanol conversion

The converted van originally used carburetion to control fuel delivery. For ease of tuning and fuel changes, the vehicle was converted to fuel injection. Because the different fuels require different amounts of delivery, a programmable fuel computer was used. A previously fuel-injected engine could use the stock computer, and increases in fuel delivery required for Aquanol could be done with increased injector size and adjusting fuel rail pressure. The programmable computer allows uploading new fuel and ignition maps when changing between fuels. Other than the catalytic igniters or spark plugs, no hardware is changed when switching fuels.

Instrumentation

While the above components are necessary for the Aquanol conversion, additional components were installed during the conversion to enhance diagnostics, and allow for data collection not available on most vehicles.

Programmable fuel injection computers must be programmed for each application. Feedback for programming is via an oxygen (O_2) sensor. Traditional sensors are very non-linear and only give feedback about whether the engine is operating rich, lean or stoichiometric. Special linear, or wide band, O_2 sensors are used to give actual values for the air/fuel ratio. This is necessary for tuning the Aquanol engine to run a constant lean mixture through all engine operation. The wide band O_2 setup can take data from four locations simultaneously. Because the van uses batch fuel injection, no individual cylinder tuning is possible. For this conversion, just a single location that samples all the cylinders was used.

A second fuel system is used on the vehicle when performing tests on the chassis dynamometer. This system is also stainless, but it is a self-regulating setup with a positive displacement fuel flow measurement. This is used to record fuel usage under steady state conditions on the chassis dynamometer and gives fuel accurate economy comparisons between the two fuels.

A non-contact vehicle speed sensor is required for taking precise, high frequency speed measurements. In order to characterize the vehicle road load, several coast down tests must be performed. The speed sensor uses radar Doppler measurements updated 100 times per second. This is logged in a laptop computer for future processing. Knowing the road load parameters is necessary to predict power usage for given speeds and road conditions. The data collected is used to pick operating points on the chassis dynamometer that mimic actual driving parameters.

3. Initial findings

The vehicle was driven several hundred miles since the initial conversion, during which some of the systems were debugged. No noticeable difference in power or performance between gasoline and Aquanol was observed by drivers. Fuel economy

for the Aquanol showed a 30 percent increase in consumption over gasoline. This is better than expected. Ethanol only has 66 percent of the chemical energy of gasoline. Aquanol also has 35 percent water, which makes no contribution to the available chemical energy. For this reason, Aquanol has only half the energy per unit volume when compared to gasoline. Initial assumptions were that when running on Aquanol the vehicle would have twice the fuel consumption. With previous Aquanol conversions, an increase in engine efficiency was observed, which partially accounts for better fuel economy than expected.

4. Vehicle Test Plan

A three-part vehicle test plan was developed to obtain quantitative results comparing the two fuels in an on-road test platform. The first and relatively simple part of the testing was to optimize fuel/ignition maps and improve vehicle drivability before more scientific tests are performed. The second part identified and acquired road load variables. The final part of the plan was chassis dynamometer testing.

A driving cycle was created as the first part of vehicle testing. A high accuracy GPS system was used to map distances and elevations of a local driving course. This data is also programmed in a vehicle simulation software package that will help predict FTP driving cycle performance. Initially, this driving cycle was used to optimize the fuel and ignition computers maps for each fuel. Once the computer was programmed, the fuel metering system was installed and tested over the same driving cycle. Once the system was integrated in to the vehicle, 10-20 driving cycles were driven and the fuel economy was averaged for the cycle for both fuels. This was to represent expected fuel economy differences in typical city driving.

Part two of the test plan was data collection of road load parameters and selection of steady state operating points for chassis dynamometer testing. The vehicle speed sensor system was installed on the vehicle and tested for accuracy. The vehicle was

taken to a flat, straight section of road at least one mile long. For vehicle roll down tests, the vehicle is accelerated to 70 mph; then the transmission is put in neutral and the vehicle is allowed to coast to below 20 mph. The speed sensing system starts gathering data at 65 mph and stops data collection at 20 mph. Runs are done in pairs going opposite directions to help cancel out any wind and road irregularity effects. A series of 10 coast-down pairs were taken. This data was used to predict coefficient of friction and drag used in the road load equation. The vehicle simulation software used the road load equation to predict power requirements for the FTP driving cycles. Running the vehicle parameters through the software allowed selection of several steady state operating points that can be used to approximate the FTP driving cycles.

The third part of the testing was to use a steady state chassis dynamometer. The fuel measurement system was installed in the vehicle again and exhaust probes were connected to the five-gas analyzer and the FTIR spectrometer. Using the operating points identified in part two, the vehicle operated at steady state at each operating point. Data on fuel consumption, air/fuel ratio, and emissions of CO, CO_2, HC, NOx, and aldehydes were recorded. The fuel was switched, and the same chassis tests performed on the second fuel.

Summary—Vehicle Testing

Catalytically assisted combustion of fuel-water mixtures represents a new paradigm for piston engine development. Instead of reducing pollutants with after-treatment systems at the expense of engine performance, the formation of pollutants is controlled at the source by chemical and gas dynamic modifications of the in-cylinder combustion process.

Catalytic igniters allow ignition of fuels not possible with conventional ignition sources. Aquanol looks to be an inexpensive, renewable fuel with distinct improvements in lowering NOx, CO, and net CO_2 emissions. By understanding what parameters effect emissions, it will be possible to make future modifications to further reduce harmful pollutants.

The demonstration platform helps promote public awareness of alternative fuels and their reduced environmental impact. The Aquanol conversion vehicle has demonstrated the potential for Aquanol fuel to be used in over-the-road platforms. Further testing will provide useful data in comparing improvements in emissions, performance, and efficiency over current gasoline platforms.

References

1. Heywood, J. (1988), *Internal Combustion Engine Fundamentals*. NY: McGraw-Hill.
2. Guerrieri, D., Caffrey, P., Rao, V. (1995), "Investigation into the Vehicle Exhaust Emissions of High Percentage Ethanol Blends," Society of Automotive Engineers Paper 950777.
3. Kelly, K., Bailey, B., Coburn, T., Clark, W., Lissiuk, P. (1996), "Federal Test Procedure Emissions Test Results from Ethanol Variable-fuel Vehicle Chevrolet Luminas," Society of Automotive Engineers Paper 961092.
4. Turns, S. (2000). *An Introduction to Combustion*. 2nd Ed, New York: McGraw-Hill.
5. Morton, A. T. (2000), "Homogeneous Charge Combustion of Aqueous Ethanol in a High Compression Catalytic Engine," MS Thesis, University of Idaho.
6. Browning, L. H., Hornborger, L. E., Likos, W. E., Mc.Cormack, M. C., and Pullman, J. B. (1977), "Characterizing and Research Investigations of Methanol and Methyl," Fuelsy ERDA contract #EY-76-S-02-1258, University of Santa Clara Report # ME-772.
7. Brinkman, N. D. (1981), "Ethanol Fuel – A Single-Cylinder Study of Efficiency and Exhaust Emissions," Society of Automotive Engineers Paper 810345.
8. Browning, L. H., Pefley, R. K. (1977), "Computer Predicted Compression Ratio Effects on NO Emissions from a Methanol Fueled S.I. Engines," Society of Automotive Engineers Paper 779006.
9. Browning, L. H., Pefley, R. K. (1979), "Kinetic Wall Quenching of Methanol Flames with Applications to Spark Ignition Engines," Society of Automotive Engineers Paper 790676.
10. Ayyasamy, R., Nagalingam, B., Ganesan, V., Gopalakrishnan, K.V., and Murthy, B.S. (1981), "Formation and Control of Aldehydes in Alcohol Fueled Engines," Society of Automotive Engineers Paper 811220.

11. Bernhardt, W. (1977), "Future Fuels and Mixture Preparation Methods for Spark Ignition Engines," *Progress in Energy and Combustion Science*, Vol. 3, pp. 139-150.
12. Pischinger, F., Kramer, K. (1979), "The Influence of Engine Parameters on the Aldehyde Emissions of a Methanol Operated Four-Stroke Otto Cycle Engine," Third International Symposium on Alcohol Fuel Technology, Asilomar, CA.
13. Samaga, B. S., and Murthy, B. S. (1976), "Investigation of a Turbulence Flame Propagation Model for Application for Combustion Prediction in the S.I. Engine" Society of Automotive Engineers 760758.
14. Lee, W., and Geffers, W. (1977), "Engine Performance and Exhaust Emissions Characteristics of Spark Ignition Engines Burning Methanol and Methanol Mixtures," A.I.Ch.E. Symposium Series #165, Vol. 73.
15. Badami, M. G., Ayyaswamy, R., Nagalingam, B., Ganesan, V., Gopalakrishnan, K. V., and Murthy, B. S. (1980), "Performance and Aldehyde Emissions of a Surface Ignition Engine and Comparison with Spark Ignition Engines," Fourth International Symposium on Alcohol Fuel Technology, Brazil.

Acknowledgements

This work was supported by funding from:
Idaho Transportation Department (ITD)
Idaho Department of Water Resources (IDWR)
Idaho Space Grant Consortium (ISGC)
US Department of Defense (DOD-EPSCOR)
US Department of Transportation, University Transportation Centers Program (UTC)
The National Institute for Advanced Transportation Technology (NIATT)

B. ENGINE TESTING AND IGNITER MODELING

Introduction

Lean burning in piston engines affords a means of achieving important environmental and fuel economy objectives. The need to overcome the difficulties related to lean burning originally spurred the development of the catalytic igniter [1]. The primary drawbacks of traditional lean burn engines are de-rated power output per unit displacement and incompatibility with oxidation/reduction catalysts used in conventional exhaust clean-up systems [2]. The catalytic igniter was devised to overcome these problems. A variety of converted engines have shown increased power output and thermal efficiency, while extending lean-burn limits, and reducing emissions [3, 4].

Over the last five years the University of Idaho along with Automotive Resources, Inc., has combined this catalytic igniter design with aqueous fuel technology to capture many of the benefits of lean burning without sacrificing power output and emissions. The fuel in this study is a mixture of 30 percent water and 70 percent ethanol. Because ethanol readily adsorbs water, no special processes are necessary to make this fuel. Previous screening tests with small spark ignition engines (less than 1000 cc) modified for aqueous fuel have indicated dramatic reductions in NOx and hydrocarbon emissions. Detailed understanding of combustion physics is necessary to successfully scale up characteristics from small, low compression engines to larger high compression engines. The modeling and experimentation efforts described in this section of the report have been undertaken to build this understanding.

Igniting aqueous fuels requires a larger ignition source than gasoline or diesel fuels. A high-energy spark can initiate ignition, but the water in the cylinder quickly extinguishes the flame. Standard compression ignition of aqueous fuels has been unsuccessful due to problems controlling ignition timing. The catalyst provides a

reliable and controllable ignition source that promotes thorough combustion of the mixture in the main chamber.

A number of research papers discuss the benefits of water mixed in fuel, including ethanol. However, successful cold starting of engines with more than 20 percent water in the fuel is not found in the literature. After warm-up without water injection, many HCCI engines require inlet air pre-heaters to continue operation after water injection begins [5-8]. Catalytic ignition is capable of cold starting engines with as much as 50 percent water in the fuel, and the energy used to heat the catalyst is minimal.

1. Catalytic Igniter Concept

The catalytic igniter is a self-contained ignition system that can be retrofitted to both spark-ignition (SI) and compression ignition (CI) engines. An exploded view of the system and its parts is illustrated in Fig. 1. The catalytic igniter consists of a ceramic rod with an embedded heating element and a coating of noble metal catalyst. Cold starting requires up to 25 watts/igniter from an external power source (12 volt). Upon reaching operating temperature, the ignition process is self-sustaining and no longer requires power from an external source. The catalytic core is enclosed in a custom-machined brass shell that forms a pre-chamber adjacent to the main combustion chamber. The shell fits into existing spark plug holes on SI engines or direct fuel injection ports on CI engines.

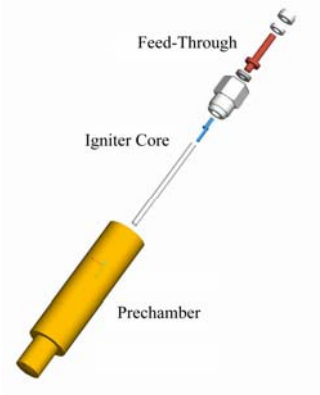

Figure 1. Exploded view of catalytic igniter

Ignition begins as fresh mixture contacts the catalyst during the compression stroke. Because of the reduced activation energy associated with heterogeneous catalysis, this occurs at temperatures far below the normal gas-phase ignition temperature [9]. Combustion products and intermediate species then accumulate in the pre-chamber surrounding the catalytic core. After sufficient temperature is achieved due to compression, multi-point homogeneous ignition results [9, 10]. The mixture is then rapidly expelled through the nozzles at the bottom of the igniter. The nozzles direct the flame to ignite the entire combustion chamber in an exceedingly short period of time. The resulting flame pattern is illustrated in Fig. 2.

Figure 2. Flame pattern exiting the nozzle of the catalytic igniter

With any homogeneous charge compression ignition engine, controlling ignition timing is a critical problem. Early experimental work explored a mechanical means of controlling catalytic ignition. Adjusting the position of the catalyst in the pre-chamber had a large effect on ignition timing. A mathematical model was created to simulate conditions in the catalytic igniter and to help conceptualize the trends observed. This model also permits parametric studies of compression ratio, catalyst surface temperature, and percent water content.

2 Catalytic Ignition Model

The first iteration of the catalytic ignition model was created to determine the sensitivity of ignition timing to various parameters. The model presented here is not meant to be predictive, but rather identifies qualitative behavior of ignition timing.

Future iterations of the model will use three-dimensional modeling and more complete reaction mechanisms to more accurately predict ignition timing and emissions.

The model uses a lumped-parameter model created by dividing the catalytic igniter into three zones [11]. In the model, each zone is assumed to be perfectly stirred (i.e., characterized by a single temperature and fuel concentration for each zone) and situated as in Fig. 3. Zone I is the pre-chamber region in front of the core. Zone II, the only zone where catalytic surface reactions take place and where electrical heating is possible, is the pre-chamber region that surrounds the catalytic portion of the core. Zone III is the pre-chamber region that surrounds the non-catalytic portion of the igniter core. Only gas-phase reactions take place in this region.

Because the total nozzle area and pre-chamber area are similar, pressure is assumed to be constant across all zones and determined by piston position. Mass is progressively transferred from Zone I through Zone III as the piston moves upward. The temperature and fuel concentrations in each zone are governed by equations of mass and energy conservation.

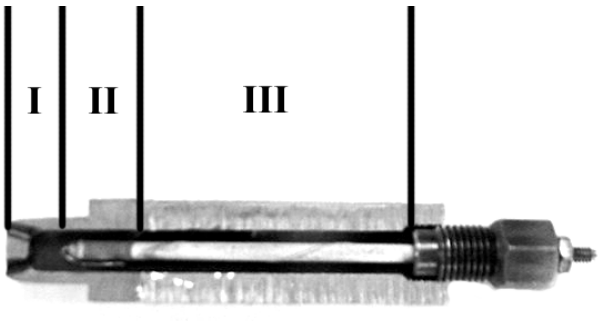

Figure 3. Igniter cut away showing zones used in model

Gas-phase ignition timing is arbitrarily defined as the crank angle when the gas-phase reaction rate exceeds the surface reaction rate. It is assumed that reactions on the

catalyst surface are mass transfer limited, and therefore nearly constant. Gas-phase reactions obey an Arrhenius relationship that increase rapidly near ignition. Shortly after gas-phase ignition, the mixture in the pre-chamber will auto ignite and torch the main chamber.

The model is an energy and mass balance in a closed system. The overall energy balance for the system is described in Eq. 1. Instantaneous temperature in each zone can be found by integrating this equation.

$$\dot{E}_{zone} = \dot{E}_{core} - \dot{E}_{wall} + \dot{E}_{comp} + \dot{E}_{trans} + \dot{E}_{\hom} + \dot{E}_{het} \quad (1)$$

Ėzone is the time rate of change of sensible energy within a particular zone. Ėcore is the heat transfer from the catalytic core element to the gas mixture. Ėwall is the heat transfer from the gas mixture to the pre-chamber wall. Ėcomp is the compressive work done on the system by the piston. Ėtrans is the sensible heating/cooling from mass transfer between zones. Ėhom is the sensible heating from homogeneous reactions. Ėhet is the sensible heating from heterogeneous reaction.

A detailed description of each term in the energy equation is given below. In the following equations "i" is an index from 1–3 indicating that the equation applies to each zone. The subscript "j" is an index that denotes particular chemical species. Ėzone can be used to determine the instantaneous temperatures in each zone. This results in Eq. 2, which is a differential equation for temperature. In this equation, m is the mass in the zone, and Cv is the average specific heat for the mixture.

$$\dot{E}_{zone\,i} = m_i C_{vi} \frac{dT}{dt} \quad (2)$$

Ėcore and Ėwall are assumed to follow a simple convection model. We chose to use an average value for the convective heat transfer coefficient (h). Surface areas, Asurf_core, and Asurf_prechamber, are the circumference of the parameter times the length of the zone. Tcore is temp of catalytic core element and T is the instantaneous

temperature of the gas mixture in the particular zone. Eqns. 3 and 4 show the formulas for Ėcore and Ėwall .

$$\dot{E}_{core_i} = h_{core} A_{surf\_core_i} \left(T_{core} - T_i\right) \tag{3}$$

$$\dot{E}_{wall_i} = h_{wall} A_{surf\_prechamber_i} \left(T_i - T_{wall}\right) \tag{4}$$

Ėcomp is assumed to follow a polytropic process. For an open system, this term is a function of the volume of each zone and the time rate of change of pressure as shown in Eq. 5. Ėtrans accounts for mass flux entering and leaving each zone. Each species concentration, specific heat, and associated enthalpy is tracked. Equation 6 shows the formula for sensible heating/cooling due to mass transfer. Ax is the cross sectional area available for mass transfer. Enthalpy H is summed over all species and is a function of instantaneous temperature. M refers to molecular weight, and c refers to concentration. v is the transport velocity. We assume that this interface velocity is a function of piston location and speed as shown in Eq. 7.

$$\dot{E}_{comp_i} = Vol_i \frac{dp}{dt} \tag{5}$$

$$\dot{E}_{trans_i} = A_{x_i} v_i \left[\sum_j H_j(T_i) M_{ji} c_{ji} - H_j(T_{i-1}) M_{ji} c_{ji} \right] \tag{6}$$

$$v = \frac{X}{L} * U \tag{7}$$

In Eq. 8, X is the location in the igniter measured from the feed through end, L is the stroke, and U is the instantaneous piston speed. In Eq. 8, θ' is the angular crank speed, θ is the crank angle, and R is the ratio of the connecting rod to crank radius.

$$U = \pi L \theta' \sin(\theta) \left[1 + \frac{\cos(\theta)}{\left(R^2 - \sin^2(\theta)\right)^{1/2}} \right] \tag{8}$$

The rates of reaction are tracked using a simplified two-step model. Ėhom represents energy liberation from a two-step reaction mechanism. These are modeled in Eq. 9. In the first step, ethanol oxidizes to H_2O and CO. In the second step, the CO is oxidized to CO_2 [12]. LHV is the lower heating value, and k is the corresponding reaction rate constant [13]. Ėhet applies only in Zone II where the catalyst is present. This describes the surface reaction. In Eq. 10 Carea is the concentration of active sites on the catalytic surface and S is a sticking coefficient that describes the statistical probability that a molecule will stick and react on the catalyst surface.

$$\dot{E}_{\mathrm{hom}_i} = M_{ethanol} k_{ethanol_i} c_{ethanol_i} LHV_{ethanol} + 2 M_{CO} k_{CO_i} c_{CO_i} LHV_{CO} \tag{9}$$

$$\dot{E}_{het_i} = \left(\frac{1}{\left(c_{area_i}\right)^m} S \sqrt{\frac{RT_i}{2\pi M_{ethanol}}} \right) \mathrm{X} M_{ethanol} \; c_{ethanol_i} LHV_{ethanol} \tag{10}$$

In order to determine reaction rates, the concentrations of species in each zone are necessary. The instantaneous species concentrations (O_2, N_2, H_2O, CO_2, CO, and C_2H_5OH) can be found by integrating the mass transfer equation. The time rate of change in concentration results in several differential equations (one for each species in each zone). The first term in the equation represents mass transfer entering the zone, and the second term is mass exiting. The third term represents generation/destruction due to chemical reactions.

$$\frac{dm_{ji}}{dt} = A_{x_{i-1}} v_{i-1} c_{ji-1} - A_{x_i} v_i c_{ji} + Vol_i \frac{dc_{ji_{react}}}{dt} \tag{11}$$

3. Model Validation

Equations outlined in the previous section were implemented numerically in a Matlab® model. Solutions began at the start of compression and proceeded until Ėhom

exceeded Ėhet. This is the definition of homogeneous ignition because Ėhom becomes nearly asymptotic as seen in Fig. 4. The crank angle where this occurs is taken as the point of gas phase ignition. The model uses parameters from the Yanmar test engine (Table 1).

TABLE 1 Original specifications for the Yanmar engine

Cylinders	3
Bore	7.5 cm
Stroke	7.5 cm
Displacement	998 cc
Compression Ratio	17.5:1
Rated Power	15 kW
Maximum Speed	3000 rpm

The model keeps track of the reaction rates in each zone as a function of crank angle and records the angle of ignition. The primary output of the model is the point of ignition and several plots of reaction rates, concentrations, and temperatures in each zone as a function of crank angle. A plot of the ratio of heterogeneous to homogeneous reaction heat release with respect to the crank angle is shown in Fig. 4.

The heterogeneous surface reaction is nearly constant and is not able to initiate ignition alone. The homogeneous reaction rate starts very low, but increases exponentially past the heterogeneous rate. It is assumed that ignition follows very shortly once the homogeneous rate exceeds the heterogeneous rate. Figure 4 shows the results when the homogeneous reaction rate was divided by the heterogeneous reaction rate at each crank angle to determine the ratio. The value of 1 on the y-axis represents when the homogeneous reaction rate exceeds the heterogeneous reaction rate. Plotted alone, the heterogeneous surface reaction rate is a nearly straight line with slight positive slope. The input conditions modeled in Fig. 4 are the physical engine geometry, an air/fuel equivalence ratio of 0.60 and an engine speed of 2000 RPM. By our arbitrary definition of ignition timing, the point of ignition can be seen at about 15 degrees before TDC.

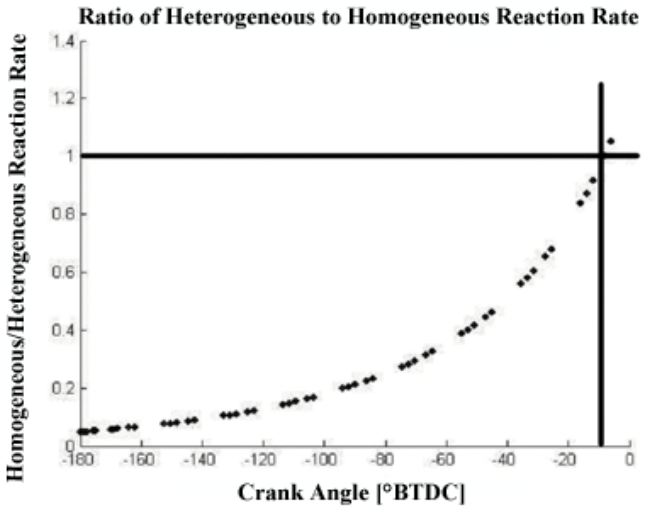

Figure 4. Sample output of model comparing the heterogeneous surface reaction and homogeneous gas-phase reaction rates

The catalytic ignition model was verified with data collected from a 15 kW Yanmar Diesel converted to operate on water-ethanol fuel using catalytic ignition. The specifications for this engine are in Table 1. Besides replacing the direct injection fuel injector with the catalytic igniter, the major changes to the engine involved fuel handling.

Catalytic ignition conversions have been done on both SI and CI engines. All of the catalytic ignition engines are homogeneous charge. Engines converted from SI platforms control load by throttling an air/fuel mixture. The air/fuel ratio remains nearly constant across all operating conditions. As such, converted SI platforms differ only in the ignition mechanism. In these engines, catalytic ignition allows the use of fuels not normally sustained by spark ignition. Engines converted from CI platforms are not throttled. In these engines, load is controlled solely by changing the amount of fuel delivered to the engine. The volume of air/fuel mixture in the cylinder remains nearly constant for all conditions, but the air/fuel ratio itself varies. However, fuel is injected in the intake manifold and allowed to mix upstream of the combustion chamber. Consequently, converted CI platforms operate in a homogeneous charge mode over a wide range of air/fuel equivalence ratios.

The Yanmar conversion described in this paper was formerly a CI engine. Common rail injection was added to the original intake manifold and controlled by a programmable fuel injection computer.

Figure 5 shows the experimental apparatus used to collect data from the converted Yanmar engine. The head on the conversion engine was modified to accept pressure transducers to obtain in-cylinder pressure readings for each cylinder. These are flush mounted in the head, but were installed through sleeves in the head cooling passages. Because of this cooling, special purpose transducers with full Envar bodies are capable of undistorted operation at the lower combustion temperatures associated with water-ethanol/air mixtures. A 1000 pulse/revolution optical encoder was used to trigger readings from the pressure transducers. This gives a reading every 0.36 degrees of crank angle. A water-brake dynamometer with computer load and fuel control was used control the engines for all tests. Pressure and crank angle were recorded with a 200 kHz data acquisition system and fed to a PC for post processing. Monitoring three cylinders allows each cylinder to collect data at 66 kHz, which is adequate for sampling up to 4000 RPM.

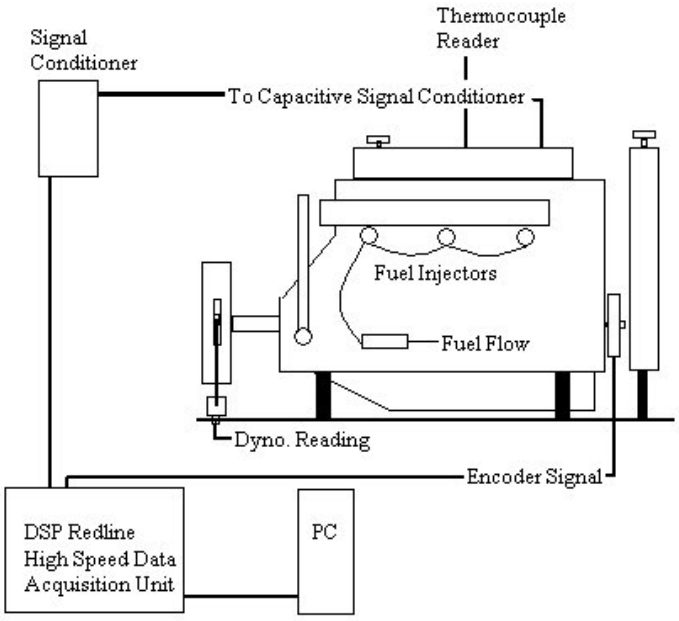

Figure 5. Experimental apparatus for Yanmar testing

A four-channel wide band air/fuel sensor is used for measuring the equivalence ratio of the mixture in the engine. Three of the sensors monitor individual cylinder mixture, while the fourth measures the average of all the cylinders after the exhaust collects. A five-gas emissions analyzer also provides redundant air/fuel ratio measurement of the total exhaust flow.

The above setup provides instantaneous pressure as a function of crank angle and air/fuel equivalence ratio measurements. Figure. 6 shows typical pressure traces of each cylinder along with a motoring trace without ignition for the converted Yanmar engine. Engine conditions for this figure are the same modeled in Fig. 4 (2000 rpm and equivalence ratio of 0.6). In Fig. 6, the axes have been cropped to show detail around the point of ignition. Actual ignition is taken as the crank angle where the pressure trace departs from the motoring trace. In this example, the ignition timing is about 17 degrees BTDC (Before Top Dead Center).

When running under lean (i.e., low load) conditions, the peak pressure is significantly lower than under high load conditions. Peak pressures under high load are over 7500 kPa.

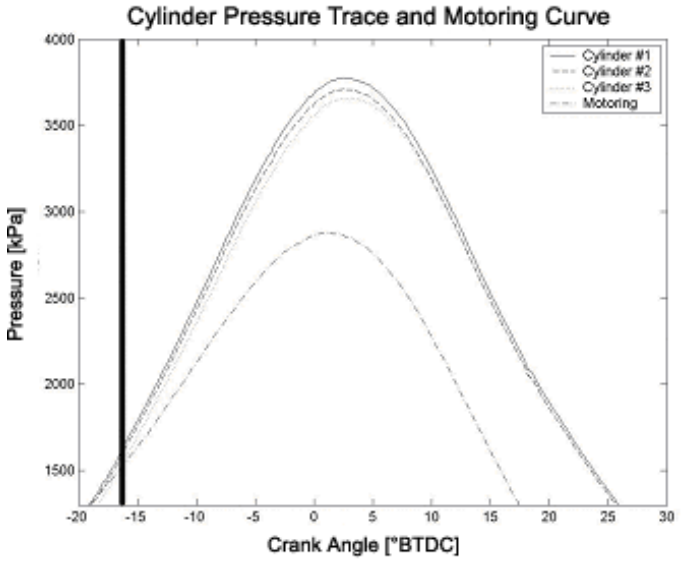

Figure 6. Ignition and motoring curves for Yanmar engine. Test conditions are the same as modeled in Fig. 4.

Data were compared with ignition timing predicted by the model. The results are shown in Table 2. Four quadrants were targeted: high-speed high-load, low-speed high-load, high-speed low-load, and low-speed low-load. For the qualitative first-order model developed here, the results follow trends similar to the actual engine.

TABLE 2 Comparison of ignition timing between model and engine pressure data

	Model	Actual
2000 RPM		
Equivalence ratio 0.6	15° BTDC	17° BTDC
Equivalence ratio 0.8	12° BTDC	13° BTDC
3000 RPM		
Equivalence ratio 0.6	17° BTDC	17° BTDC
Equivalence ratio 0.8	10° BTDC	12° BTDC

This was the first of several planned iterations on a catalytic ignition model. Refining the mass transfer between regions is necessary for a more accurate assessment of species concentration. Some variables like the convection coefficient should be a variable of velocity instead of an averaged constant value. Similarly, investigating radiation heat transfer and how it affects ignition timing will be considered. The model would also benefit from more detailed reaction chemistry. This would allow us to optimize the igniter for other types of fuels. This model will eventually expand to include gas dynamics in the igniter as well as the main chamber

4. Parametric Studies

Sensitivity studies on the parameters affecting ignition timing are valuable in guiding future generations of catalytic igniter designs. Empirical data shows changes in igniter length, catalyst surface temperature, and compression ratio impact ignition timing. The model described here allows the user to rank the relative importance of these parameters. Results from parametric studies are shown in Table 3. The parametric studies were performed around parameter values representing the current design.

These ranges were:

Igniter length	38–50 mm
Surface temperature	700–1500 K
Compression ratio	6.0 – 22.0 CR
Water content	0–50 percent water by vol.

TABLE 3 Results of modeling parametric study

Parameter	Sensitivity	Units
Igniter length	5.58	°BTDC/mm
Surface temperature	0.54	°BTDC/K
Compression ratio	0.27	°BTDC/CR
Water content	0.00	°BTDC/%water

Changing igniter core length changes the crank angle where the fresh mixture first contacts the catalytic surface. Until recently, this was the main means of controlling the ignition timing in the converted engines. However, this does not allow for ignition advance at increasing engine speeds. Typically ignition timing should advance with engine speed, and retard with load so that peak pressure is reached at or shortly after TDC.

Altering surface temperature controls the rate of reaction on the catalyst. The higher the catalyst temperature, the earlier ignition will occur. Currently surface temperature is not regulated. For cold starting and idle conditions a constant power of 25 watts/igniter is supplied to heat the catalytic surface. At higher speeds and loads the catalytic surface retains enough heat to be self-sustaining without electric heating. The parametric study shows that controlling the catalyst temperature has potential for improved ignition control.

Dynamically changing compression ratio is not feasible for most engines without significant modifications. However, because conversions are done on both CI and SI engines, knowing how compression ratio effects ignition timing will help create the

right geometry for the various engines that will be converted. Currently, igniters for high compression ratio engines are much shorter than low compression ratio engines, which agree with the model predictions.

The catalytic igniters have successfully demonstrated cold start operation and supported combustion of ethanol-water mixtures up to 50 percent water. Dynamic control of water content would be possible if the fuel and water were handled in separate injection systems. While there might be other benefits in the areas of emissions or combustion efficiency, changing water concentration appears to have an insignificant effect on ignition timing. However, water content will have an effect on the rate of combustion after the onset of ignition.

5 Engine Performance

To further evaluate the performance and emissions of catalytic ignition with ethanol-water fuel, two 15 kW Yanmar diesel engines were acquired. Both were rebuilt and tuned, and neither was equipped with exhaust cleanup devices. One was left in stock condition, while the other was converted to catalytic operation. Changes made to the converted engine were:

- Replacing diesel injectors with catalytic igniters;
- Adding programmable common rail fuel injection to the intake manifold;
- Machining cylinder head for pressure sensors; and
- Milling the head to maintain the same compression ratio as the stock engine because of the additional volume of the catalytic pre-chamber.

Both engines were tested using the same protocol. Full possible RPM sweeps were done at constant throttle settings between 50 percent and 100 percent in 5 percent increments. Engine Speed, Corrected Power, Torque, Fuel Flow Rate, Exhaust Velocity, Exhaust Temperatures, Air/Fuel Ratio, and Concentrations of O2, NOx, CO, CO_2, and HC data was recorded.[10] to make comparisons of the two engines under a multitude of operating conditions.

Comparisons of Brake Mean Effective Pressure (BMEP) and corrected shaft power for the two engines are shown in Figs. 7 and 8. Because of faster pressure rise in the cylinder from combustion of a homogeneous mixture, the conversion engine displays an increase in BMEP over all engine speeds. Improvements over the stock configuration at full load ranged from 9 percent to 33 percent in BMEP and maximum power.

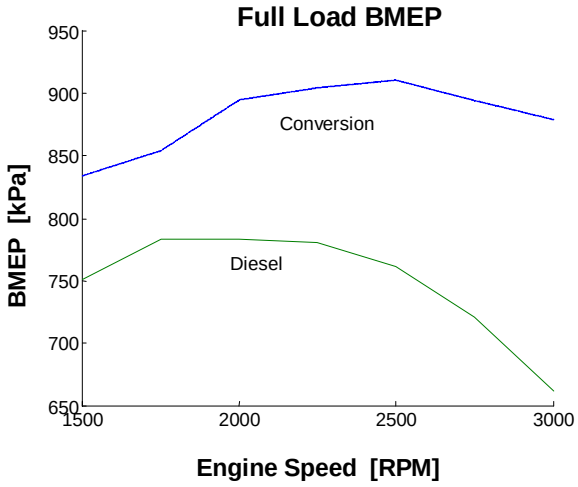

Figure 7. Comparing BMEP of the diesel and converted engines

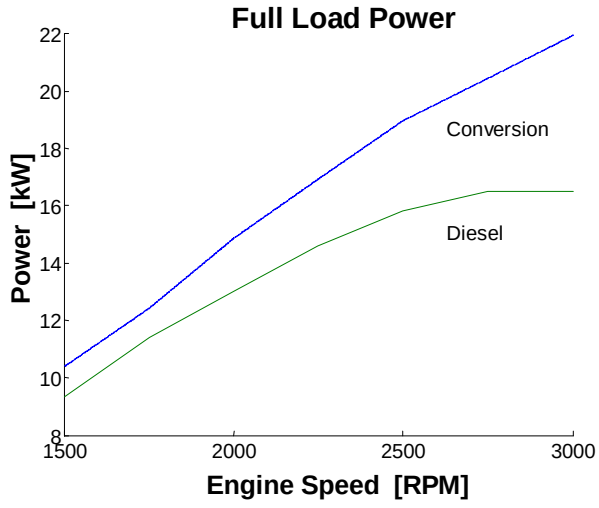

Figure 8. Comparing power of the diesel and converted engines

The stock engine was not designed for operation over 3000 RPM. In stock configuration, this is controlled by diffusion limitations. However, the converted engine does not suffer this limitation. The homogeneous mixture in the converted engine combusts much faster than the diesel engine. For safety reasons, the engine management computer was programmed to cut fuel past 3000 RPM. Without this limitation, increased engine speeds have potential for further power gains. Rotating assemblies will require modification to safely operate at higher speeds.

It seems counter-intuitive that the ethanol-water converted engine would produce more power. This is possible because the flow rate of fuel is much greater for ethanol-water than diesel. At full power, the diesel engine operates lean, but because of the slow diffusion burn, there is not adequate time to combust any additional fuel. The homogeneous charge ethanol-water engine, on the other hand, produces peak power operating slightly rich (equivalence ratio of 1.1). The heating value of the 70–30 ethanol-water mixture is calculated at 17.4 MJ/kg, making it 42 percent lower than diesel fuel at 41.4 MJ/kg [14]. Because of this, comparisons of net indicated efficiency are used to compare two engines. Net indicated efficiency is defined as engine power divided by the product of the mass flow rate of fuel and the heating value of the fuel. These comparisons are given in Tables 4–7.

For ease of comparison, four zones of operation were targeted to display results. Engine speeds of 1750 RPM and 2750 RPM were chosen to represent low and high speed operation. BMEP values of 500 kPa and 720 kPa were chosen for high and low load points. These four points were within the operating ranges of both engines.

TABLE 4 Emissions and efficiency at 1750 RPM and 500 kPa

	Diesel	Conversion
Indicated efficiency	23.4%	25.5%
BSCO [gm/kW*hr]	29.4	14.7
BS CO_2 [gm/kW*hr]	271	798
BSNOx [gm/kW*hr]	2.03	0.421
BSHC [gm/kW*hr]	0.031	10.6

TABLE 5 Emissions and efficiency at 2750 RPM and 500 kPa

	Diesel	Conversion
Indicated efficiency	33.4%	22.3%
BSCO [gm/kW*hr]	4.3	12.6
BS CO_2 [gm/kW*hr]	449	1010
BSNOx [gm/kW*hr]	3.79	0.376
BSHC [gm/kW*hr]	0.0478	5.63

TABLE 6 Emissions and efficiency at 1750 RPM and 720 kPa

	Diesel	Conversion
Indicated efficiency	27.1%	42.1%
BSCO [gm/kW*hr]	29.4	11.9
BS CO_2 [gm/kW*hr]	254	728
BSNOx [gm/kW*hr]	2.48	0.478
BSHC [gm/kW*hr]	0.0572	7.32

TABLE 7 Emissions and efficiency at 2750 RPM and 720 kPa

	Diesel	Conversion
Indicated efficiency	28.6%	38.4%
BSCO [gm/kW*hr]	19.3	11.3
BS CO_2 [gm/kW*hr]	404	652
BSNOx [gm/kW*hr]	424	0.265
BSHC [gm/kW*hr]	0.0279	6.79

The stock diesel engine has a maximum efficiency of 35 percent around 2000 RPM and between 50 percent and 90 percent of maximum torque. However, at higher loads, the net indicated efficiency is in the range of 23 percent to 28 percent. The converted engine has a higher maximum efficiency of 42 percent, but this occurs over a narrower speed range, around 1750 RPM and between 70 percent and 80 percent of maximum torque. Under full load conditions the efficiency of the converted engine ranges from 32 percent to 35 percent. Net indicated efficiency for the converted engine is lower under low-load conditions where the air/fuel mixture is very lean, and the flame is easily quenched. Poor combustion efficiency is likely the cause of lower efficiency and higher emissions in this operating range.

6 Emissions

Improving engine efficiency and reducing undesired exhaust emissions is the ultimate goal of this research. At this stage, we have demonstrated an increase in net indicated efficiency, with improvements in several exhaust species. However, there is still more work necessary to curb HC and CO emissions. Data was collected on brake-specific emissions of CO, CO_2, NOx, and HCs for both engines. The results are displayed in Tables 4-7 above.

Carbon monoxide emissions were highly dependant on engine operating conditions. The stock diesel engine has a distinct minimum in the mid-load, high-speed range, but CO emissions increase significantly outside of this range. The converted engine has minimum CO at the higher loads, but has greater CO emissions than the diesel at low loads. The high CO emissions at low load are likely due to incomplete combustion of the lean mixtures. However, due to the water-gas shift mechanism, extra water present in combustion helps reduce CO emissions at higher loads.

CO_2 is a greenhouse gas, but it is important to note that ethanol is a biofuel. Because biofuels absorb CO_2 in their life cycle, the net global production of CO_2 from burning a biofuel is much lower than from a fuel pumped from the ground. The converted engine showed a notable increase in tailpipe emissions of CO_2 when compared to the diesel engine. Ethanol-water mixtures have similar carbon content per unit mass as diesel fuels. However, for similar power output, the converted engine is using almost twice the amount of fuel.

Studies on water injection to reduce NOx have been done since the 1970s. Water present in combustion helps keep combustion temperatures down, hence leading to decreased thermal NOx formation. The converted engine shows an order of magnitude reduction in NOx emissions over all ranges. Low levels of NOx are atypical for an engine with 17:1 compression ratio. In the converted engine, this is associated with a significant reduction in the exhaust gas temperature. Maximum NOx concentrations

for the converted engine were barely over 100 ppm, with minimums being below the detection threshold 10 ppm. NOx reduction without after treatment was a primary goal of this research.

Hydrocarbon emissions typically indicate unburned fuel. Because of the nature of a direct injection diesel, low HC emissions are expected, particularly under low load and speed conditions. As mixtures become closer to stoichiometric, diesel engines tend to produce greater HC emissions. The stock Yanmar engine never emitted more than 30 ppm HC. HC from the converted engine are very high, even for an HCCI engine. Peak values were nearly two orders of magnitude greater than the diesel engine at 2700 ppm. This would suggest that there is a significant amount of fuel not being burned in the combustion chamber. This is due to excessive quenching.

The pistons in both engines are inverted bowls designed for direct injection diesel combustion. The top of the piston that is not bowled gets closer to the head than the quench distance, and does not allow the air/fuel mixture in this region to ignite. Another concern is the formation of aldehydes that are byproducts of ethanol combustion. These register as HC's on the measurement equipment. Hydrocarbons are simple to clean up with modern after treatment, but significant improvements can be made in-cylinder to reduce HC emissions. Changing piston design in the converted engine to one more typical of a homogeneous charge engine shows promise in lowering HC emissions before exhaust cleanup.

Conclusion

Catalytically assisted combustion of fuel-water mixtures represents a new paradigm for piston engine development. Instead of reducing pollutants with after-treatment systems at the expense of engine performance, the formation of pollutants is controlled at the source by chemical and gas dynamic modifications of the in-cylinder combustion process.

The catalytic combustion process studied in this research consists of the following steps:

- Catalytic surface oxidation during the compression stroke at temperatures far below the normal gas phase ignition temperature;
- Accumulation of combustion products and active radicals in a small volume adjacent to the catalyst;
- Multi-point, compression ignition of gas mixture in the pre-chamber surrounding the catalyst near top dead center; and
- Rapid torch ignition of the fuel/air mixture in the main chamber.

Our catalytic ignition model represents the first three steps in this combustion process. Model predictions qualitatively agree with in-cylinder pressure data collected from a 15 kW Yanmar engine converted for catalytic operation. Our long-term goal is to expand this ignition model to include all four steps in the combustion process. The model has provided valuable insights about what parameters can be used to effectively and efficiently control ignition timing.

Catalytic igniters allow ignition of fuels not possible with conventional ignition sources. While the initial drive was for reduced emissions, an increase in power density and torque are possible using this technology coupled with ethanol-water fuel. This is done while increasing overall engine efficiency, but requires increased fuel flow and storage capacity. Modifications to further increase combustion efficiency are

underway. Replacing the bowl pistons with shorter flat top pistons is expected to reduce the quench area on the converted engine. This should significantly reduce HC emissions.

The original goal of reducing NOx in lean burn, high compression engines has been realized in the current conversion. In this research, it is important to remember that that no after treatment has been used to clean the exhaust emissions. The goal has been to control emissions at the source. There is still room for improvement of CO and HC emissions. Future in-cylinder modifications promise to reduce these emissions, which can also be easily cleaned up with original equipment from the banufacturer after treatment systems.

References

1. Cherry, M., "Catalytic-Compression Timed Ignition," U.S. Patent 5 109 817, December 18, 1990.
2. Cherry, M., Morrisset, R., and Beck, N., "Extending Lean Limit with Mass-Timed Compression Ignition Using a Plasma Torch," Society of Automotive Engineers Paper 921556, 1992.
3. Gottschalk, Mark A., "Catalytic Ignition Replaces Spark Plugs," *Design News*, May 22, 1995.
4. Dale, J. and Oppenheim, A., "A Rationale for Advances in Technology of IC Engines," Society of Automotive Engineers Paper 820047, 1982.
5. Browning, L. H., and Pefley, R. K., "Kinetic Wall Quenching of Methanol Flames with Applications to Spark Ignition Engines," Society of Automotive Engineers Paper 790676, 1979.
6. Pischinger, F., and Kramer, K., "The Influence of Engine Parameters on the Aldehyde Emissions of a Methanol Operated Four-Stroke Otto Cycle Engine," Third International Symposium on Alcohol Fuel Technology, Asilomar, CA, May 28-31, 1979.
7. Lee, W., and Geffers, W., "Engine Performance and Exhaust Emissions Characteristics of Spark Ignition Engines Burning Methanol and Methanol Mixtures," A.I.Ch.E. Symposium Series #165, Vol. 73, 1977.
8. Christensen, M., and Johnasson, B., "Homogeneous Charge Compression Ignition with Water Injection," Society of Automotive Engineers Paper 1999-01-0182, 1999.
9. Cho, P. and Law, C., "Catalytic Ignition of Fuel/Oxygen/Nitrogen Mixtures over Platinum," *Combustion and Flame*, Vol. 66, pp. 159-170, 1986.
10. Pfefferle, L., "Catalysis in Combustion, Catalysis Reviews," *Science and Engineering*, Vol. 29, pp. 219-267, 1987.
11. Clarke, E., "Characterization of Aqueous Ethanol Homogeneous Charge Catalytic Compression Ignition," Masters Thesis, University of Idaho, 2001.

12. Westbrook, C. K., and Dryer, F. L., "Simplified Reaction Mechanisms for the Oxidation of Hydrocarbom Fuels in Flames," *Combustion Science and Technology*, Vol. 27, pp. 31-43, 1981.
13. Coltrin, M., Kee, R., Rupley, F., and Meeks, E., "Surface Chemkin III," Sandia National Laboratories, SAND96-8217, 1996.
14. Heywood, J. B. *Internal Combustion Engine Fundamentals*. New York, McGraw-Hill, 1988.

Acknowledgments

This work was supported by funding from:
Idaho Transportation Department (ITD)
Idaho Department of Water Resources (IDWR)
Idaho Space Grant Consortium (ISGC)
US Department of Defense (DOD-EPSCoR)
US Department of Transportation, University Transportation Centers Program (UTC)
National Institute for Advanced Transportation Technology

C. ETHANOL-WATER COMBUSTION KINETICS

1 Catalytic Reactor – Mixing Nozzle Evaluation

The schematic for the plug flow reactor under construction is displayed in Figure 1. The vaporization and mixing sections are complete. The reaction section will consist of a quartz-lined steel tube where plug flow is established for catalytic reactions.

The major feature of the mixing section is a mixing nozzle designed to quickly and evenly blend two gas streams. To test how quickly the nozzle operated, two gas streams were plumbed to the nozzle: one of nitrogen, and the second of a calibration gas (Table 1). Solenoid valves controlled the proportion of total flow attributed to each gas stream. An electrochemical cell gas analyzer monitored flow at different axial and radial downstream positions. The analyzer could sense carbon dioxide, carbon monoxide, nitrogen oxide, oxygen, and unburned hydrocarbons.

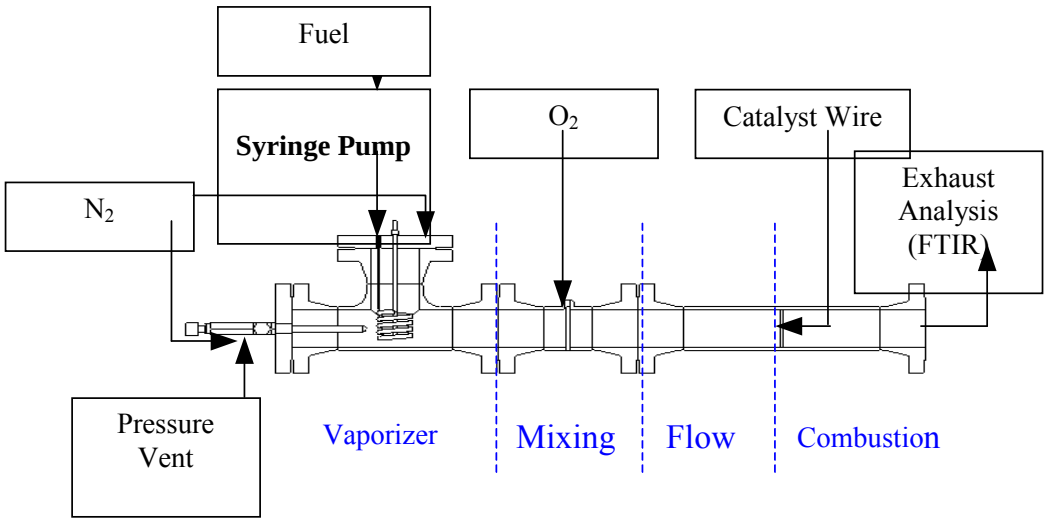

Figure 1. Schematic of the plug flow reactor.

Calibration gas was introduced to both of the mixing nozzle inlets until the flow composition in the reaction section reached steady state. The flow composition was then abruptly altered by the use of solenoid valves to dilute the calibration gas by 50 percent by switching one inlet gas stream to pure nitrogen. Little axial variation was observed (Fig. 2), although the time for the system to respond—15 seconds—was far too long for practical purposes.

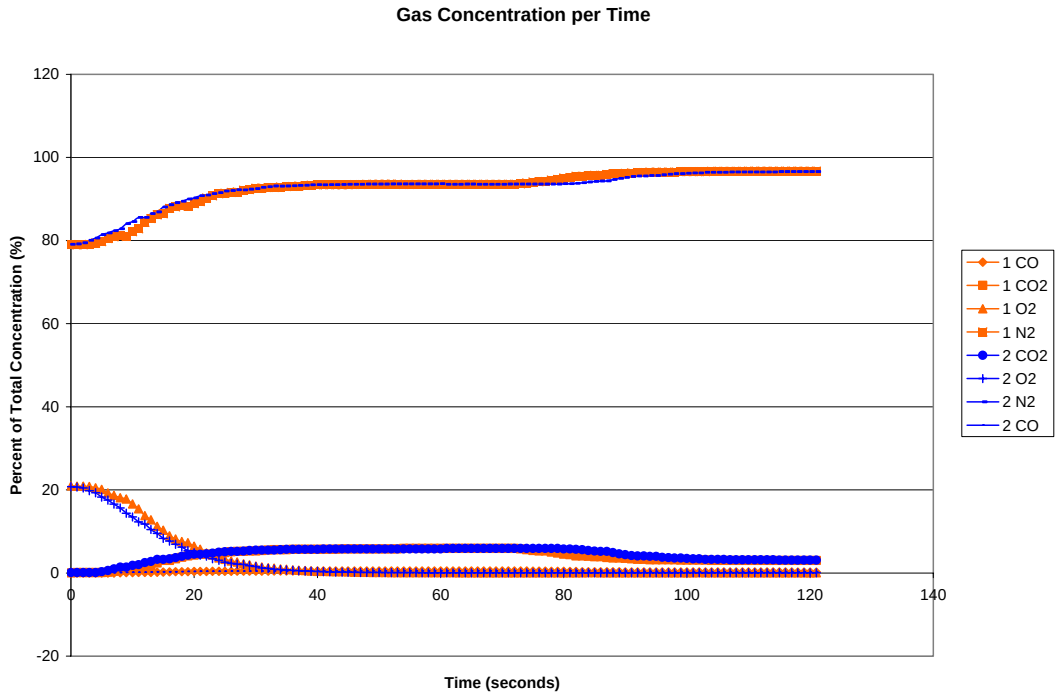

Figure 2. Flow composition in the reaction section at position 1 (1/2 diameters) and position 2 (10 diameters) downstream from the mixing nozzle. The indexer used to locate axial positions is shown in Fig. 4.

TABLE 1 Composition of test gases

Calibration Gas Tank	Nitrogen Tank
HC 202 PPM	N2 100 percent
NO 298 PPM	
NOx 300 PPM	
CO 0.5 percent	
CO_2 6.5 percent	
N2 Balance	

To identify the cause of this delay and decrease it, three possible causes of the delay in response time were isolated:

1. Diameter of the probe
2. Length of the probe
3. Flow rate of the gas

Tests were performed to determine which factor played the most significant role in slowing the response time. Changes one and two were made at the exhaust end of the reactor and the flow rate was adjusted by varying the pressure from the gas tanks. Gases from two fifteen-gallon tanks were flowed through the flow meters shown in Fig. 3 below.

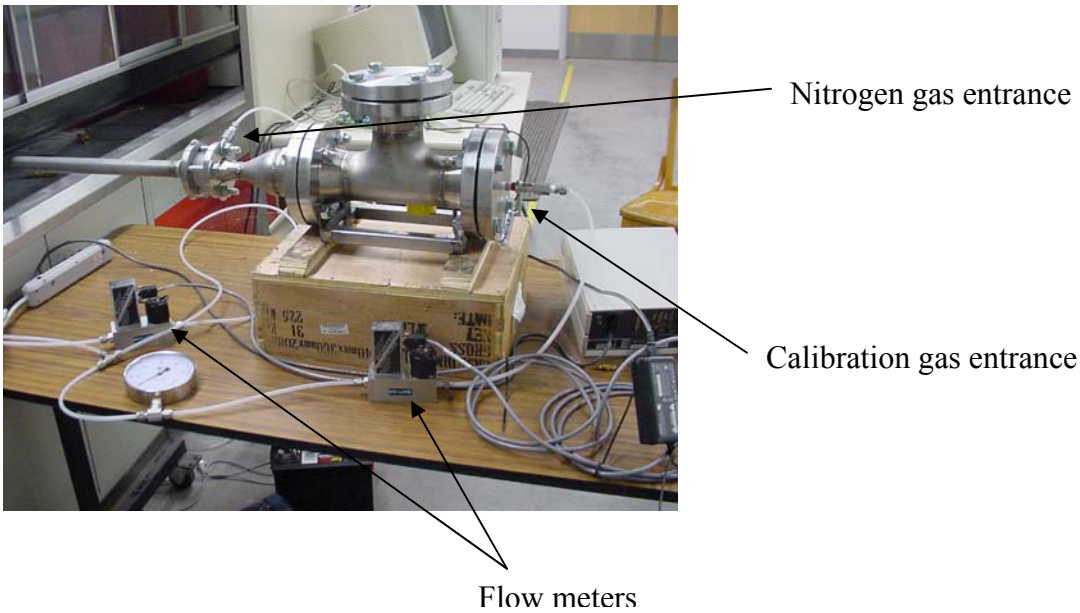

Figure 3: Reactor setup shown from the flow meter side. The mixing nozzle is held between the two flanges where the nitrogen stream is introduced for the nozzle response tests.

Calibration and nitrogen tank gas entered the reactor as shown in Fig. 3. From this point, the gas proceeded through the mixing nozzle and to the probe located in the exhaust pipe. This probe is connected to the gas analyzer used to collect data.

In testing for the first possible cause, the diameter of the probe, the standard hypo tubing (of inner diameter 1 mm) was replaced with vinyl tubing (inner diameter 0.3125 inch). The calibration gas was turned on and elapsed time was measured until the gas analyzer indicated the change. Seventy seconds later (after the exhaust gas concentration reached equilibrium) the nitrogen gas was turned on and, again, elapsed time was recorded.

Figure 4. Indexer inserted into the reaction section to locate repeatable axial locations for gas sampling

At first the results obtained seemed to show a large decrease in response time. Concentrations began changing in the gas analyzer after only four or five seconds. Further investigation into the data, however, revealed a different trend. By comparing the new results to those from the fifteen-second response data, it was determined that there was little difference in when the change was detected. The difference was in the quickness of the change (the slope of the concentrations). The setup was modified to record not only the time until initial response from the gas analyzer but also concentration changes over time recorded in five-second intervals.

This procedure was performed for sampling probe lengths of 35 and 101 inches. The flow rate was kept constant at 13.2 percent total for the calibration gas and 16.4 percent total for the nitrogen. This corresponds to a volumetric flow rate of about 43 cm3/sec. The variation of sampling probe length had no effect on the response time.

To determine the effects of changing the gas flow rate, pressure was increased through the flow meters from 50 to 100 psi. Doubling the pressure resulted in a 62 percent increase in volumetric flow for the calibration gas and a 72 percent increase for the nitrogen. Response times were slightly affected: The response time lapse dropped from an average 4.9 seconds at 50 psi to an average 4.0 seconds at 100 psi. Nitrogen response fell by a similar amount.

The next step was to obtain velocity profile measurements across the diameter of the exhaust pipe at incremental locations from the nozzle. A hotwire anemometer was calibrated for use with the gases used. The purpose of these tests is to map out the "plug" flow section, the axial range where the radial velocity profile varies by no more than 10 percent of the mean velocity.

2 Modeling Gas Phase Combustion of Ethanol-Water-Air Mixtures with HCT

The chemical kinetic's code HCT (hydrodynamics, combustion and transport) developed by Lawrence Livermore National Laboratory was used to model gas-phase combustion of ethanol-water-air mixtures. HCT will be modified to accommodate surface reactions, and thus be available as a tool for better understanding of catalytic ignition of aqueous ethanol.

The gas-phase reaction mechanism that we are using is based on the model of Norton and Dryer [1992]. At first, they also used HCT to calculate chemical kinetics of ethanol. The model was developed after conducting a series of ethanol combustion experiments. The results included product composition as a function of time, product composition changes with fractional fuel consumption, net reaction rate with the changes of fractional fuel consumption, in a plug flow reactor. The simulation was compared with their experimental results and found consistent.

It is important to understand that the elementary reactions and parameters in combustion are subject to ongoing research and updating as new information becomes established. It is beyond the scope of our research plan to add to this body of knowledge. Rather, we strive to keep abreast of new discoveries for implementation in our research.

There are at least two other ethanol combustion mechanisms, and it is worthwhile to discuss the most recent, that of Marinov [1998]. Marinov also accepted the initial ethanol decomposition concept that Borisov [1991] and Norton and Dryer [1992] used. Basically, the initial decomposition of ethanol in combustion can follow one of three parallel paths, depending on which of three H-atom bonds in ethanol are broken first. The subsequent temperature-dependent product distribution during the combustion is developed with 372 elementary reactions. Marinov used the combustion kinetics code Chemkin to test his mechanism. He found good results with his mechanism when compared with experimental data from Natarajan and Bhaskaran [1981], of ignition delay in shock tubes from Gulder [1982], of laminar burning velocities in freely propagating flames from Aboussi [1991] and Dagaut [1992], the latter referred to the Aboussi data set in their ethanol oxidation modeling study, in modeling species concentrations in a jet-stirred reactor, and from Norton and Dryer [1992] in species concentrations from a plug-flow reactor.

The comparison between experimental data from a variety of apparatuses and combustion conditions with Marinov's model is good enough to suggest that the mechanism is a general one of high accuracy. However, included with the mechanism are reaction parameters for elementary reactions that are presented for the first time. Despite the good agreement with the mechanism and published data, these parameters (the pre-exponential constant, temperature dependency, and activation energy) are currently subject to further investigation by the combustion community.

In contrast, the Norton and Dryer [1992] ethanol combustion mechanism contains 142 elementary reaction equations. The forward and reverse reaction parameters they published have not been changed substantially by other combustion chemists.

HCT, using HCTPLT to plotting, now runs in a PC Windows operating system. Preliminary results, using the Norton-Dryer mechanism for 100 percent ethanol in air burning in a plug-flow reactor, show that the simulation is too fast compared with published experimental data. There are several possibilities for this error, and we are working closely with HCT authors and users at LLNL to understand why and to find a correction.

For example, after we rechecked the input file for errors mistyping the ethanol mechanism parameters and flow reactor boundary conditions, researchers at LLNL suggested different boundary conditions. This change also returned combustion rates that were too fast in comparison to experimental data.

Also, when given the forward reaction rate constants in the input file, HCT can be requested to calculate reverse reaction rate constants using detailed balancing. These constants differed substantially from those published in the Norton and Dryer mechanism. When reverse reaction rate parameters were entered independently and HCT instructed not to calculate reverse reaction constants (thus making HCT “see” the reversible 142 reaction mechanism a forward-only mechanism with 284 reactions), the simulated combustion rate was far too slow in comparison with published data. Not all of the elementary reactions are reversible, however, and the remaining task is to check all the input file settings that flag each reaction’s characteristics.

We doubt there are operational issues with the copy of HCT that we are using and believethat the problem lays in the input data. We made several modifications to the code before it could be compiled without errors. The HCT code includes three parts: MKCDAT, to form a database of reaction rate parameters and thermodynamic

properties for running HCT; HCT, to run the core reaction mechanism; and HCTPLT, for plotting results. MKCDAT and HCT are available for either PC or UNIX systems; we used only the PC version.

Once we got the MKCDAT code, we deleted portions of the code automatically produced in a UNIX platform. The modified program passed through the compilation and linking process with our PC FORTRAN compiler, finally forming one executive file MKCDAT.exe.

We also worked with the HCT part following the same approach we used in MKCDAT. Despite receiving a PC version, we faced modifications due to differences between FORTRAN for UNIX and FORTRAN for PC Windows. Furthermore, while originally compiling the HCT code, we found calls to subroutines that did not exist. All of the missing pieces of code were mathematical subroutines from one a popular library, BLAS. We downloaded the subroutines from a BLAS support website and ran them with HCT. To gain confidence that these were indeed the correct missing subroutines, we also took subroutines with same names from the UNIX version of HCT, with the same result.

We reached the conclusion that our copy of HCT worked correctly, despite subroutine modifications, by reproducing a published example problem [Lund, 1995]. The example was for ozone formation and destruction. With only three species (O_3, O_2 and O) and three reactions, the ozone mechanism was simple to check. We reproduced the published results for species concentration and temperature variation with time. The only problem we encountered was the calculation for the laminar flame speed. The copy of HCT we had did not use the same model for the laminar flame speed as that used for the published example. We investigated different laminar flame speed models [Turns, 2001 and Lund, C. M., 1995] and found three that produced results similar to the original, unknown model, and in the HCTPLT source code. We adapted these three models for the plotting of laminar flame speed.

Finally, we are still working to streamline the operation of the plotting part, HCTPLT. Of the three parts of the HCT package, HCTPLT was never ported from UNIX to a PC platform. HCTPLT uses the NCARG and GKS libraries to plot. These two libraries were first developed for the UNIX system as graphics libraries. A Slovenian professor, Dr. Milan Batistain at the University of Ljubljana, modified the NCARG and GKS system using Compaq Visual FORTRAN for PC Windows use. It will be more efficient to get the modified graphing subroutines working with HCTPLT instead of writing our own plotting package from scratch. Hence, we are now also using Compaq Visual FORTRAN.

At first, all the HCT source was modified using Lahey FORTRAN. When we nearly finished all the modification of MKCDAT and HCT code by this FORTRAN compiler, we continued our work of HCTPLT. We found that Lahey FORTRAN cannot run the NCARG and GKS libraries correctly, so transferred to Compaq Visual FORTRAN.

Finally, two significant research tasks remain. First, we need to develop the surface reaction mechanism for the ethanol-water-air-Pt system. Second, we need to include surface reactions by adding subroutines to MKCDAT and HCT, and thus create the HCTS (HCT Surface) code. We are gradually developing our surface mechanism and have finished some parts.

3 Catalytic Reaction Mechanisms

An oxidative catalyst on the surface of an igniter promotes stable ignition of lean fuel-air mixtures. The catalyst not only increases the rate at which chemical reactions (combustion) take place but also decreases the minimum temperature needed for the reactions to take place. If the heated igniter surface can be used as a catalyst for ignition, lower temperatures would be required, thus increasing the lifetime of the igniter as well as reducing the energy requirements for proper operation.

There is no general consensus on the mechanism of catalytic oxidation reactions in the literature [Spivey, et al., 1987]. Depending on specific catalyst and hydrocarbons studied, different mechanisms have been proposed.

Other researchers have looked at the use of oxidative catalysts for igniting hydrocarbons mixed with water in air. Beld, et al. [1995] studied the complete oxidation of ethane, propane and their mixtures on a Pd/Al2O3 catalyst, investigated the effect of the reaction products on the kinetics, and found that whereas water significantly retards oxidation, the influence of CO_2 is negligible under the pressure (160-500 kPa) and temperature (450-475K) ranges explored. Although these conditions are not the same as those expected for the catalytic igniter that we are studying, it is interesting to learn that water acts to inhibit fuel oxidation. Reynaldo, et al. [1991] studied the feasibility of igniting methanol in a two-stroke diesel engine with the assistance of a combustion catalyst glow plug. The author concluded that the platinum catalyst used did not deteriorate with use, a welcome conclusion because of the similarity of their experiment with our research.

Several researchers have studied low-temperature catalytic reactions of ethanol. While it is useful to be aware of this research, specific results are not applicable to the high-temperature mechanism we expect in our work.

Jelemensky, et al. [1996] developed a kinetic model for the platinum catalyzed oxidation of ethanol. The reaction mechanism he developed is a sequence of proposed steps for the selective oxidation of aqueous ethanol with molecular oxygen. While developing the model, the author also considered three types of oxygen species, at least two of them being active for the oxidations. He concluded that both the interconversion of these species and their reactivity towards the adsorbed ethanol is strongly dependent on the state of the catalyst. The experiment was performed under a total pressure of 600 kPa and a temperature of 323 K. It is clear that the low temperature tests to convert aqueous ethanol to other species is for chemical

manufacturing, not combustion, and is of little value to us. The author provides some useful insights of catalytic ethanol oxidation, however.

Davidson, et al. [1987] studied thermal decomposition of ethanol vapor over a Pd/Al2O3 catalyst, and used the Langmuir-Hinshelwood-Hougen-Watson (LHHW) method to derive a number of trial kinetic rate equations based on surface reaction rates of adsorbed species and the appropriate adsorption-desorption pseudo-equilibria. Then by fitting these equations, they obtained steady-state isothermal differential rates of thermal decomposition of ethanol to $CH_4/CO/H_2$ via the intermediate ethan0l (CH_3CHO). The LHHW is not the same method we will use for our surface reaction mechanism because the reaction is at 479K, far lower than about 1100K.

The LHHW model subdivides the overall process of gas-solid reactions into the following three constituent processes:

1. Two molecules adsorb onto the surface.
2. They diffuse across the surface and interact when they are close.
3. A molecule is formed which desorbs.

The LHHW models for the catalytic decomposition of ethanol is as follows, giving the rate of H2 and CH4 formation:

$$r_{H_2} = \frac{k_5 \left(P_{C2H5OH} - P_{CH3CHO} P_{H2} \Big/ K_e \right)}{\left(1 + K_6 P_{CH3CHO} P_{H_2} + K_8 P_{CO} + K_{10} P_{H2} + K_{11} P_{CH4}\right)}$$

$$r_{CH4} = \frac{K_7 K_8 P_{CH3CHO}}{\left(1 + K_6 P_{CH3CHO} P_{H_2} + K_8 P_{CO} + K_{10} P_{H2} + K_{11} P_{CH4}\right)^n},$$

where the detailed number of parameters, such as kn, can be found in the paper the author published in 2001, and Pi are the partial pressures of species i. Again, we benefit from mechanism insights and rate-determining steps. This is the second paper we found about catalyzed ethanol reactions.

Gardiner [1972] subdivided the overall process of heterogeneous reactions into the following five consecutive steps:

1. Transport of the reactant molecule to the surface by convection and/or diffusion;
2. Adsorption of the reactant molecule on the surface;
3. Elementary reaction steps involving various combinations of adsorbed molecules, surface sites, and gas-phase molecules;
4. Desorption of product molecules from the surface;
5. Transport of the product molecules away from the surface by convection and/or diffusion.

Our heterogeneous model for oxidative catalysis of ethanol-water-air over Pt.

Miessen, et al. [2001] investigated the oxidation of graphite as a model for the combustion of char. Numerically, they studied the stagnation-point flow of an oxygen stream on a graphite surface. They modeled the chemical reactions including gas-phase as well as the surface reaction part. In the model, they also considered the interactions of gas-phase modules with surface complexes, the different surface complexes formed and the influence of the geometry of the graphite surface. Like many papers from the Interdisciplinary Center for Scientific Computing (IWR) of the University of Heidelberg, the author provided information regarding how to write surface reaction mechanisms step by step. In this model, the authors considered the effect of nitrogen and products of combustion including carbon monoxide and carbon dioxide.

Anotonello, et al. [1993] investigated the reaction mechanism of ethanol over platinum in order to identify the reaction path. Certainly it is a preliminary step useful for the reduction of the effect required for discrimination between different reaction rates and for parameter evaluation. The knowledge of the reaction mechanisms is also useful for analysis and prediction of the behavior of catalytic combustion of ethanol-contained

mixtures that cannot be simply inferred from the behavior of the single compounds. With these preliminary researches, we can write the ethanol surface reaction mechanism on the Pt catalyst. From experimental data, we can obtain the surface reaction parameter for these reactions.

Using a stagnation-point flow model with detailed gas-phase, surface kinetics and transport using an arc-length continuation technique, Bui et al. [1997] studied the catalytic ignition of H2/air mixtures over platinum surface. This research is very useful for us to help understand the fundamental catalytic surface reactions. In contrast, the research reported by Deutschmann and Warnatz [2002] follows several steps: first, design an experiment; collect experimental data; use their simulation tool DETCHEM to simulate the experiment; if the model they developed is in good agreement with the experimental data, they conclude that their surface reaction model is correct. What is missing in their research is in-depth theoretical analysis. The theoretical analysis should be more involved than simply developing one model, simulating it, comparing it with the experiment data, plotting several graphics, and claiming that their model is correct. The potential problem is that there are many possibilities that could result in good agreement between simulation and experimental data. Although we remain skeptical about the veracity of their model until other researchers verify it's applicability, their work is very helpful for our research.

Huff [2000] studied the role of gas-phase reactions in Pt-catalyzed conversion of ethane-oxygen mixtures in monolith reactors. A multi-step heterogeneous mechanism is employed along with a homogeneous mechanism in plug flow to simulate the result of an ethane oxidative de-hydrogenation experiment. The author's conclusion indicates that all of the ethylene produced in the simulations originates from endothermic gas-phase reactions, the heat for which is provided by catalytic ethane oxidation. Unfortunately, heat conduction in the reactor wall is not modeled accurately in the plug flow analysis. Zerkle [2000] indicates that such simplifications have a dramatic effect on the calculated peak wall temperature. Huff gives us some clues to

study the hydrocarbon heterogeneous reaction mechanism further and catalytic hydrocarbon combustion in plug flow, both of which are also useful for our research.

Zerkle, et al. [2000] performed research about homogeneous and heterogeneous contributions to the Pt-catalyzed partial oxidation of ethane in a short-contact-time reactor. In the research, Zerkle employed detailed homogeneous and heterogeneous chemical kinetic mechanisms to describe the chemistry. In the heterogeneous mechanism, there are totally 82 reactions. The rate constants for these elementary surface reactions are determined through a combination of literature sources, theoretical estimates, and fitting to experiment data. The potential issue in his heterogeneous reaction mechanism is that the rate constants from fitting are based on little experiment data. More experimental data is needed for the rate constants for elementary surface reactions to be accurately decided. Zerkle's ethane mechanism provides many useful elementary surface reactions for our research, and more thoughts about the Pt-cataytic combustion mechanism for methanol and ethanol.

Daniel, et al. [2001] developed a two-dimensional flow field model, including a detailed reaction mechanism, for the conversion of CO, C3H6, O2, and NO to simulate the exhaust gas treatment in a platinum/rhodium-coated single channel of a typical three-way converter. This research is directed at the automotive industry and their use of 3-way catalytic converters (for the reduction of NO, and the oxidation of CO and unburned hydrocarbons) to clean up exhaust gas. The authors developed a complete model, a reliable multi-step reaction mechanism, which includes 61 reactions and 31 species. In the complete model, the author considered two sub-models: the C3H6 elementary model and the NO formation model. The reaction mechanism includes many reactions useful for use to begin writing an ethanol combustion model on Pt catalyst. In our model there are undecided parameters left that we will to find either through our own experiments or progress from other research groups. Gradually, our ethanol mechanism will be complete.

The research group of Dr. J. C. Warnatz has published more than 50 papers about catalytic combustion and surface reactions. Fortunately, we have received all of their published papers and carefully read them. Their research direction is not always the same as ours. Some of their research conclusions are useful; some of them are in other directions, such as char, which helps us only by studying their method. Regardless, their research is very helpful for us, although there are some missing pieces.

In summary, with the help of so many references that we have checked, we have a solid foundation to begin describing the ethanol surface reaction mechanism on the Pt catalyst. The research group under the leadership of Dr. J. C. Warnatz, which has been conducting surface reaction research for nearly ten years, has published the most information regarding individual surface reactions. As a graduate student in the field of surface reaction ten years ago, Dr. Olaf Deutschmann finished the program DETCHEM used it to run Warnatz's surface reaction models. Other surface reaction tools, 1-D and 2-D models supported by the CFD tool FLUENT, we do not have the resources to obtain or modify. Fortunately, with the HCT code, the many research reports about surface reaction mechanisms, and the heterogeneous reaction algorithms in programs such as CHEMKIN and DETCHEM, we can gradually finish our surface reaction program HCTS.

4 The HCTS (HCT-Surface) Program

Numerical methods for the surface reaction mechanisms named the Chemkin Collection [Coltrin M. E., 1995] and DETCHEM [Deutschmann O., 1996], respectively, have been developed mainly at two institutes, Sandia National Laboratory and the Interdisciplinary Center for Scientific Computing (IWR) in University of Heidelberg. While comparing those papers published by these two institutes, we found that the theory in these two programs is basically the same. The model used by DETCHEM is more reasonable. Because we already have the main program HCT, we want to incorporate the surface reaction mechanism into it as a

subroutine rather than write a new program. The key points of the DETCHEM algorithm are explained below.

The following boundary conditions for the species governing equations is for chemical reactions on solid surfaces:

$$\eta F \dot{s} M_i = \left(\dot{j} + \rho Y_i u \right) \left(i = 1, ..., N_g \right),$$

where $\dot{j}$ the diffusion flux; Y_i the mass fraction of species i in the gas phase adjacent to the surface; u the Stefan velocity; F the ratio between catalytic active surface area and geometric surface; and η the effectiveness factor to account for pore diffusion.

Surface reactions in catalytic combustion can be considered according to methods very similar to those for gas-phase reactions when adsorbents are regarded as randomly distributed on the surface. In other words, conditions where the mean field approximation remains valid. The surface is idealized, that is, considered as being uniform. Local conditions such as edges, defects, terraces, and different structures, are not taken into account. The state of a catalytic surface can be described by temperature, T, and a set of surface coverages, Θ_i. Both parameters depend on location.

The production rates $\dot{s}_i$ of surface and gas phase species (due to adsorption and desorption) [Deutschmann O, and Warnatz J, 1996] are then written as

$$\dot{s}_i = \sum_{k=1}^{K_s} \nu_{ik} k_{fk} \prod_{i=1}^{N_g + N_s} \left(c_i \right)^{\nu'_{ik}},$$

where, K_s represents the total number of surface reactions including adsorption and desorption, ν_{ik}, ν'_{ik} equals stoichiometric coefficients, k_{fk} equals forward rate constant,

$N_g(N_s)$ equals number of gaseous (surface) species, and c_i represents the concentration of species i, which is given in $mol \cdot cm^{-2}$ for adsorbed species. Here c_i equals the surface coverage (Θ_i) multiplied by surface site density (Γ).

This formula is very similar to the one used in gas-phase reactions [Lund, 1995]. During the source code stage, we can consider it as the same formula while considering more reactants and products. We can use one or two subroutines specifically to describe the gas-phase reactions, and/or surface reactions.

However, the binding states of adsorption on the surface vary with the surface coverage of all adsorbed species [Deutschmann O, and Warnatz J, 1996]. This is very different physically from gas-phase reactions, as is seen in the added complexity in the modified Arrhenius expression for the forward rate constant:

$$k_{fk} = A_k T^{\beta_k} \exp\left[\frac{-E_{ak}}{RT}\right] \prod_{i=1}^{N_s} \Theta_i^{\mu_{ik}} \exp\left[\frac{\varepsilon_{ik}\Theta_i}{RT}\right]$$

where A_k = pre-exponential factor, β_k = temperature exponent, E_{ak} = activation energy of reaction k, and the parameters μ_{ik} and ε_{ik} describe the dependence of the rate coefficients on the surface coverage of species i. Compared with the rate constant formula used for gas-phase reactions, we also can find they are similar. Hence, the differences also can be expressed in a few subroutines, then added to the original subroutines in the HCT code.

Furthermore, for adsorption reactions, sticking coefficients are used [Deutschmann O, and Warnatz J, 2000]. The relationship between the reaction rate constant for adsorption and the sticking coefficient is given as:

$$k_{fk}^{ads} = \frac{S_i^0}{\left(1 - S_i^0 / 2\right) \cdot \Gamma^{\tau}} \sqrt{\frac{RT}{2\pi M_i}},$$

where S_i^0 = initial sticking coefficient, Γ = surface site density, in mol/cm2, τ = number of sites occupied by the adsorbing species, and M_i = molar mass of species i.

Surface coverage [Deutschmann O, and Warnatz J, 1996] is expressed as:

$$\theta_i = \frac{c_i \sigma_i}{\Gamma}$$

In general, we only need to study the steady state of catalytic reaction system, though the mechanism used in the catalytic combustion can be easily extended to study transient problems. In the steady state, the time variation of surface coverage (Θ_i) is zero:

$$\frac{\partial \Theta_i}{\partial t} = \frac{\dot{s}_i}{\Gamma} = 0 \quad \left(i = N_g + 1, ..., N_g + N_s\right).$$

This algebraic equation system is solved by a pseudo-time integration of corresponding ODE system until a steady state is reached. An implicit method based on LSODE, Livermore Solver for Ordinary Differential Equations, which solves initial value problem for stiff or non-stiff systems of first ODES, is used for time integration. An analytical Jacobian can be automatically generated from the surface reaction mechanism. The coverage data of the former iteration is used as initial conditions for the next step.

The main differences between homogeneous reactions and heterogeneous reactions are explained by these four expressions. Hence, modifications to the HCT and MKCDAT programs are also centered around these four expressions. These modifications include defining more parameters in the HCT program and adding several subroutines to form

one database specially used for surface reaction. In the modified MKCDAT program, the constant parameters used in surface reactions will be written to the database of thermodynamic properties and reaction rate constants developed for HCT.

In HCT program modification, we will develop input files like those used for gas-phase reactions: set some parameters to default values within HCT, and use the input file to change them based on different conditions. Based on the four expressions above, we need to set many subroutine interfaces to transfer parameters specially used in the surface reactions to those now used for the general gas-phase reaction. This avoids the modification of HCT on a grand scale. Hence, it is clear that the main work focus will remain on HCT modification.

REFERENCES

1. Aboussi, B., Ph.D. Dissertation, University of Orleans, France, 1991.
2. Agama, J. R., Abata, D. L., and Mullins M. E., "Catalytic ignition of methanol in a diesel engine with a platinum-coated glow plug," *Society of Automotive Engineers Transactions*, Vol. 100, Sec 3, pp. 1443-1450, 1991.
3. Barresi, A. A., "Reaction mechanisms of ethanol deep oxidation over platinum catalyst," Chem. Eng. Comm, Vol. 123, pp 17-29, 1993.
4. Behrendit, F., and Deutschmann, O. and Ruf, B., "Simulation of heterogeneous reaction systems," in: *Gas Phase Chemical Reaction Systems: Experiment and Models*, *100 years after Max Bodenstein*. Wollfrum J., and H. R. Volpp, Eds., Springer Series in Chemical Physics, pp 265-278, 1996.
5. Beld, L. and van der Ven, M. C., "A kinetic study of the complete oxidation of ethane, propane and their mixtures on Pd/Al2O3 catalyst," *Chem. Eng. Proc*. Vol. 34, pp 469-478, 1995.
6. Borisov, A.A., Zamanskii, V.M., Lisyanskii, V.V., and Rusakov, S.A. "High-temperature methanol oxidation". *Sov.J.Chem.Phys*., Vol.9, No.8, pp 1836-1849, 1992a.
7. Borisov, A.A., Zamanskii, V.M., Konnov, A.A., Lisyanskii, V.V., Rusakov, S.A., and Skachkov, G.I. "A mechanism of high-temperature ethanol ignition". *Sov.J.Chem.Phys*. Vol. 9, pp 2527-2537, 1992b.
8. Bui, P. A. and Vlachos, D. G., "Modeling ignition of catalytic reactors with detailed surface kinetics and transport: Oxidation of H2/air mixtures over platinum surfaces," *Ind. Eng. Chem. Res*., Vol. 36, pp 2558-2567, 1997.
9. Chatterjee, D., Deutschmann, O, and Warnatz, J., "Detailed surface reaction mechanism in a three-way catalyst," *Faraday Discuss*., Vol. 119, pp 371-384, 2001.
10. Coltrin, M. E., Surface Chemkin-III: A Fortran package for analyzing heterogeneous chemical kinetics at a solid surface --- gas-phase interface, Sandia Report SAND96-8217, Sandia National Laboratories, 1995.

11. Curran, H. J., Dunphy, M. P., Simmie, J. M., Westbrook, C. K., and Pitz, W. J., "Shock tube ignition of ethanol, isobutene and MTBE: experiments and modeling," Twenty-Fourth International Symposium on Combustion, The Combustion Institute, p 769, 1992.
12. Dagaut, P., Cathonnet, M. and Boettner, J. C., "A Kinetic Modelling Study of Propane Oxidation in JSR and Flame" J Chem Phys, Vol. 89, pp 867-884, 1992.
13. Davidson, J. M., and McGregor, C. M., "The kinetics of palladium-catalyzed vapor-phase thermal decomposition of ethanol," *Ind. Eng. Chem. Res.*, Vol. 40, pp 101-107, 2001.
14. Deutschmann, O., Schmidt, L. D. and Warnatz, J., "Detailed modeling of short contact-time-reactors," ECCE2-Second European Congress of Chemical Engineering Montpellier 1999.
15. Deutschmann, O., 'Catalytic combustion: state of the art and modeling needs,' 2nd International workshop on Chemkin in Combustion, Edinburgh, Scotland, July 30, 2000.
16. Deutschmann O., Behrendt, F., and Warnatz, J., 'Modeling and simulation of heterogeneous oxidation of methane on a platinum foil,' *Catalysis Today*, Vol. 21, pp 461-470, 1994
17. Deutschmann, O., and Schmidt, R., "Numerical modeling of catalytic ignition," Twenty-Sixth Symposium (International) on Combustion, The Combustion Institute, pp 1747-1754, 1996.
18. Deutschmann, O., and Warnatz J., "Diagnostics for Catalytic Combustion," Chapter 20 in *Applied Combustion Diagnostics*, Kohse-Hoeinghaus, K., and Jeffries, J.B., Eds., pp 518-533, Tayolr and Francis, 2002
19. Dryer, F. L., High Temperature Oxidation of Carbon Monoxide and Methane in Turbulent Flow Reactor, AMS Report T-1034, 1972.
20. Dunphy, M.P. and Simmie, J. M., "High-temperature oxidation of ethanol part I," *J Chem Soc Faraday Trans*, Vol. 87, pp 1691-1695, 1991.
21. Dunphy, M.P. and Simmie, J. M., "High-temperature oxidation of ethanol part II," *J Chem Soc Faraday Trans*, Vol. 87, pp 2549-2559, 1991.

22. Egolfopolous, F. N., Du, D. X. and Law, C. K., "A study of ethanol oxidation kinetics in laminar premixed flames, flow reactors, and shock tubes," Twenty-Fourth Symposium (International) on combustion, The Combustion Institute, pp 883, 1992.
23. Gardiner, W. C., Jr., *Rates and Mechanism of Chemical Reactions*, Benjamin, Menlo Park, CA, 1972.
24. Guider, O. L., "Laminar Burning Velocities of Methanol, Ethanol, and Isooctane-Air Mixtures," Nineteenth Symposium (International) on Combustion, The Combustion Institute, p 275, 1982
25. Hindmarsh, A. C., "ODE pack, a systematized collection of ODE solvers," in: *Scientific Computing*, R. S. Stepleman, North-Holland, Amsterdam, pp 55-64, 1983
26. Huff, M. C., Androulakis, I. P., and Sinfeit, J. H., {} *J. Catal*. Vol. 191, 2000
27. Jelemensky L., Kuster, B. F. M. and Marin, G. B., "Kinetic modeling of multiple steady-state for the oxidation of aqueous ethanol with oxygen on a carbon supported platinum catalyst," *Chem. Eng. Sci*., Vol. 51, No. 10, pp 1767-1776, 1996.
28. Kee, R. J., Rupley, F. M., and Miller, J. A., Chemkin-III: A Fortran Chemical Kinetics Package for the Analysis of Gas Phase Chemical Kinetics, Sandia Report #SAND 89-8009; Sandia National Laboratories, 1995.
29. Larson, R. S., A Fortran Program for the analysis of plug flow reactors with gas-phase and surface chemistry, Sandia Report #PLU-036-2, 2001.
30. Lund, C. M. and Chase, L., HCT A general Computer Program for calculating time-dependent phenomena involving one-dimensional hydrodynamics, transport, and detailed chemical kinetics, UCRL-52504, 1995.
31. Marinov, N. M., "A detailed chemical kinetics model for ethanol oxidation," Western States Section/ Combustion Institute, Spring Meeting, 1997.
32. Marinov, N. M., "A detailed chemical kinetic model for high temperature ethanol oxidation," *International Journal of Chemical Kinetics*, Vol. 31, No. 3, pp 183-220, March, 1999.

33. Miessen, G., Behrendt, G., Deutschmann F. O. and Warnatz J., "Numerical studies of the heterogeneous combustion of char using detailed chemistry," *Chemophere*, Vol. 42, pp 609-613, 2001.
34. Natarajan, K., and Bhaskaran, K. A., "An experimental and analytical investigation of high temperature ignition of ethanol," Nineteenth Symposium (International) on Combustion, The Combustion Institute, p 384, 1981.
35. Norton, T. S. and Dryer, F. L., "An experimental and modeling study of ethanol oxidation kinetics in an atmospheric pressure flow reactor," *Int. J. Chemical Kinetics*, pp 179-185, 1990
36. Norton, T. S. and Dryer, F. L., "The flow reactor oxidation of C1-C4," Twenty-Third Symposium (International) on Combustion, The Combustion Institute, p 384, 1981
37. Spivey, J. J., "Complete catalytic oxidation of volatile organics," *Ind. Eng. Chem. Prod. Res. Dev*., Vol. 26, pp 2165-2180, 1987.
38. Tischer, S., Correa, C., and Deutschmann, O., "Transient three-dimensional simulation of a catalytic combustion monolith using detailed models for heterogeneous and homogeneous reactions and transport phenomena," *Catalysis Today*, Vol. 69, pp 57-62, 2001.
39. Turns, S. R., *An Introduction to Combustion: Concepts and Applications*, McGraw-Hill, Inc., 2001.
40. Zerkle, D. K., Allendorf, M. D., and Wof, M., "Understanding Homogeneous and Heterogeneous Contributions to the Platinum-Catalyzed Partial Oxidation of Ethane in A Short Contact Time Reactor," *J. Catal*. Vol. 196, pp 18-39, 2000.

FINDINGS; CONCLUSIONS; RECOMMENDATIONS

Catalytically assisted combustion of fuel-water mixtures represents a new paradigm for piston engine development. Instead of reducing pollutants with after-treatment systems at the expense of engine performance, the formation of pollutants is controlled at the source by chemical and gas dynamic modifications of the in-cylinder combustion process.

Catalytic igniters allow ignition of fuels not possible with conventional ignition sources. Aquanol looks to be an inexpensive, renewable fuel with distinct improvements in lowering NOx, CO, and net CO_2 emissions. By understanding what parameters effect emissions, it will be possible to make future modifications to further reduce harmful pollutants.

A demonstration platform will help promote public awareness of alternative fuels and their reduced environmental impact. The Aquanol conversion vehicle has demonstrated the potential for Aquanol fuel to be used in over-the-road platforms. Further testing will provide useful data in comparing improvements in emissions, performance, and efficiency over current gasoline platforms.

The catalytic combustion process studied in this research consists of the following steps.

1. Catalytic surface oxidation during the compression stroke at temperatures far below the normal gas phase ignition temperature;
2. Accumulation of combustion products and active radicals in a small volume adjacent to the catalyst;
3. Multi-point, compression ignition of gas mixture in the pre-chamber surrounding the catalyst near top dead center; and
4. Rapid torch ignition of the fuel/air mixture in the main chamber.

Our catalytic ignition model represents the first three steps in this combustion process. Model predictions qualitatively agree with in-cylinder pressure data collected from a 15 kW Yanmar engine converted for catalytic operation. Our long-term goal is to expand this ignition model to include all four steps in the combustion process. The model has provided valuable insights about what parameters can be used to effectively and efficiently control ignition timing.

Catalytic igniters allow ignition of fuels not possible with conventional ignition sources. While the initial drive was for reduced emissions, an increase in power density and torque are possible using this technology coupled with ethanol-water fuel. This is done while increasing overall engine efficiency, but requires increased fuel flow and storage capacity. Modifications to further increase combustion efficiency are underway. Replacing the bowl pistons with shorter flat top pistons is expected to reduce the quench area on the converted engine. This should significantly reduce HC emissions.

The original goal of reducing NOx in lean burn, high compression engines has been realized in the current conversion. In this research, it is important to remember that that no after treatment has been used to clean the exhaust emissions. The goal has been to control emissions at the source. There is still room for improvement of CO and HC emissions. Future in-cylinder modifications promise to reduce these emissions, which can also be easily cleaned up with original equipment from the manufacturer after treatment systems.

The design and construction of the reactor is well underway. A prototype mixing nozzle has been tested for gas-stream mixing and flow characterization.

Good progress has been made in the understanding of the gas phase and surface reactions of ethanol. The physical equations needed to incorporate surface reactions into the HCT code have been identified.